

EFFECTS OF COCHANNEL INTERFERENCE
ON MSK AND OQPSK SIGNALS IN
SATELLITE CHANNELS

CENTRE FOR NEWFOUNDLAND STUDIES

TOTAL OF 10 PAGES ONLY
MAY BE XEROXED

(Without Author's Permission)

VARGHESE PHILIP



EFFECTS OF COCHANNEL INTERFERENCE ON MSK
AND QPSK SIGNALS IN SATELLITE CHANNELS

By

□ Varghese Philip, B.E.



A thesis submitted to the School of Graduate Studies
in partial fulfillment of the requirements
for the degree of
Master of Engineering

Faculty of Engineering and Applied Science
Memorial University of Newfoundland

January, 1984

St. John's

Newfoundland

Canada

ABSTRACT

The implementation of frequency-reuse techniques and sharing of the same frequency band with terrestrial microwave networks have increased the levels of cochannel interference in satellite communication systems. In fact, in certain situations such an interference can become the dominant factor in limiting the system performance. In this thesis, we analyze the effect of cochannel interference on the error rate performance of MSK and OQPSK signals transmitted through a satellite channel.

The satellite channel is assumed to exhibit both amplitude and phase nonlinearities. The system model assumed a sufficiently large bandwidth so that the intersymbol interference may be neglected. Narrowband Gaussian noise is assumed on both links but the cochannel interference is considered only in the uplink.

The bit error rate expressions are derived for MSK and OQPSK signalling techniques in the form of infinite series containing double integrals. The effect of multiple cochannel interference is evaluated using these expressions. A simple expression which does not contain infinite series is also derived for evaluating the bit error rate when only one cochannel interferer is present. The effect of the TWT input

power backoff on the bit error rate is also analyzed. The error rate expressions are evaluated over a range of uplink and downlink signal to noise ratios.

The following conclusions are drawn from this study:

- (a) MSK is superior to OQPSK for all uplink and downlink signal to noise ratios for hard-limited and TWT channels.
- (b) The optimum operating region is the saturation region for both signalling schemes.
- (c) The hard-limiter model is a good replacement for the TWT model for low uplink SNR for both the signalling techniques.

ACKNOWLEDGEMENTS

The author wishes to express his sincere gratitude to Dr. N. Ekanayake for his enthusiastic supervision and valuable guidance during the entire course of this work. Sincere thanks are also due to Dr. G. R. Peters, Dean of Engineering and Applied Science and Dr. T. R. Chari, Associate Dean of Engineering and Applied Science for their help and encouragement.

The author is indebted to Dr. F. A. Aldrich, Dean of Graduate studies for awarding a university Fellowship. The assistance and helpful suggestions provided by S. K. Srivastava, M. A. Marshall and Wayne Raman-Nair are also appreciated. The author is also thankful to Levinia Vatcher for typing the manuscript.

TABLE OF CONTENTS

	Page
ABSTRACT	ii
ACKNOWLEDGEMENTS	iv
TABLE OF CONTENTS	v
LIST OF TABLES	vii
LIST OF FIGURES	viii
NOMENCLATURE	x
CHAPTER 1 INTRODUCTION	1
1.1 General	1
1.2 Quadrature-carrier Modulation Techniques	2
1.3 Cochannel Interference	8
1.4 Literature Review	10
1.5 Outline of the Thesis	12
CHAPTER 2 BIT ERROR RATE EXPRESSIONS FOR MINIMUM SHIFT KEYING SIGNALS	14
2.1 Introduction	14
2.2 System Model	15
2.3 Decision Circuit Input	17
2.4 Probability of Bit Error	21
2.4.1 Conditional Probability of Bit Error	21
2.4.2 Joint Probability Density Function $p(x,y)$	23
2.4.3 Evaluation of the Moments of the Random Variables α, β	27
2.4.4 Expression for Bit Error Probability	30
2.5 Probability of Error with Single Cochannel Interferer	32
2.6 Probability of Error in the Absence of Cochannel Interference	35
2.7 Gaussian Approximation	36
CHAPTER 3 BIT ERROR RATE EXPRESSION FOR OFFSET QUADRATURE PHASE-SHIFT KEYING SIGNALS	39
3.1 Introduction	39
3.2 Decision Circuit Input	40

	<u>Page</u>
3.3 Probability of Bit Error	42
3.3.1 Conditional Probability of Bit Error	42
3.3.2 Joint Probability Density Function $p(x,y/q_1)$	43
3.3.3 Joint Probability Density Function $p(x,y)$	45
3.3.4 Expression for Bit Error Probability	47
3.4 Probability of Bit Error in the Presence of Single Cochannel Interferer	49
3.5 Probability of Bit Error in the Absence of Cochannel Interference	51
3.6 Gaussian Approximation	53
CHAPTER 4 NUMERICAL INVESTIGATIONS AND RESULTS	54
4.1 Introduction	54
4.2 Channel Models	54
4.2.1 Travelling Wave Tube Model	54
4.2.2 Hard-Limiter Model	55
4.3 Computational Details	57
4.3.1 General	57
4.3.2 Downlink Carrier Power	60
4.4 Performance of MSK and QPSK Signals in the Absence of CCI	61
4.5 Performance of MSK and QPSK Signals in the Presence of one CCI	64
4.5.1 Hard-limited Channel	64
4.5.2 TWT Channel	67
4.5.3 Comparison of Hard-limiter Model and TWT Model	78
4.6 Error Performance in the Presence of Multiple Cochannel Interferers	78
4.6.1 Exact Method	79
4.6.2 Gaussian Approximation Method	79
CHAPTER 5 CONCLUSION	83
5.1 Contributions of This Thesis	83
5.2 Recommendations for Further Research	85
REFERENCES	87
APPENDIX A	89

LIST OF TABLES

<u>Table</u>	<u>Title</u>	<u>Page</u>
4.1	Comparison of BER's of MSK, through TWT channel with backoff 0 dB, computed using $f^2(R)$ without approximation and with approximation to $f^2(q_0)$	62

LIST OF FIGURES

<u>Figure</u>	<u>Page</u>
1.1(A) QPSK Modulator	5
1.1(B) Alignment of Data Streams In Offset QPSK	5
1.2. MSK Waveforms	7
1.3 Phase Changes in MSK, Offset QPSK and QPSK	9
2.1 Model For A Satellite Communication System	16
3.1 Baseband Waveform of the Quadrature Channel From $t = -2T$ to $t = 2T$	46
4.1 Phase and Amplitude Characteristics of TWT [Thomas et al. (1974)]	56
4.2 Hard-Limiter Transfer Function	58
4.3 Bit Error Probability of MSK Signals; Hard-Limited Channel, CCI-10dB	63
4.4 Bit Error Probability of OQPSK Signals; Hard-Limited Channel, CCI-10 dB	65
4.5 Bit Error Probability of MSK Signals; TWT Channel, CCI -10 dB, Backoff 0 dB	69
4.6 Bit Error Probability of MSK Signals; TWT Channel, CCI -10 dB, Backoff -2 dB	70
4.7 Bit Error Probability of MSK Signals; TWT Channel, CCI -10 dB, Backoff -4 dB	71
4.8 Bit Error Probability of MSK Signals; TWT Channel, CCI -10 dB, Backoff -6 dB	72
4.9 Bit Error Probability of OQPSK Signals; TWT Channel, CCI -10 dB, Backoff 0dB	74
4.10 Bit Error Probability of OQPSK Signals; TWT Channel, CCI -10 dB, Backoff -2 dB	75
4.11 Bit Error Probability of OQPSK Signals; TWT Channel, CCI -10 dB, Backoff -4 dB	76

FigurePage

- | | | |
|------|---|----|
| 4.12 | Bit Error Probability of OQPSK Signal: TWT Channel, CCI -10 dB, Backoff -6 dB | 77 |
| 4.13 | Exact Bit Error Probability of MSK in the Presence of Multiple CCI; Hard-Limited Channel, CCI -20 dB | 80 |
| 4.14 | Approximate Bit Error Probability of MSK in the Presence of Multiple CCI; Hard-Limited Channel, CCI -20 dB. | 81 |

NOMENCLATURE

A_K	Amplitude of the K^{th} interferer
a_k	Binary data for $k=0,1,2,\dots$
$b_{i,m}$	Coefficients of the power series of the Characteristic function
$c(t)$	Cochannel interference
$E[\]$	Expectation of a variable
$\text{erf}(\)$	Error function
$\text{erfc}(\)$	Complementary error function
$f(\)$	AM-AM nonlinearity
$\overline{f^2(R)}/2$	Average downlink carrier power
$g(\)$	Generating function
H	Number of cochannel interferers
$H_m(\)$	m^{th} Hermite polynomial
$I_P(\)$	n^{th} order modified Bessel function of the first kind
$J_n(\)$	n^{th} order Bessel function of the first kind
$n'(t)$	Uplink Gaussian noise
$n''(t)$	Downlink Gaussian noise
$p(\)$	Probability density function
P_e	Probability of error
P_e'	Conditional probability of error
$p(x,y)$	Joint probability density function of x and y
$p(x,y/a,\beta)$	Joint probability density function of x and y conditioned on a and β
$r(t)$	Input to the detector
$S_i(t)$	Input signal to the bandpass nonlinearity

T	Bit period
t_0	Sampling instant
$\delta(\cdot)$	Dirac-delta function
ρ_u^2	Uplink SNR
ρ_d^2	Downlink SNR
σ_u^2	Uplink noise variance
σ_d^2	Downlink noise variance
θ_k	Random phase of the k^{th} interferer
$\psi(\cdot)$	AM/PM nonlinearity
ω_c	Carrier angular frequency
$\phi(u,v)$	Joint characteristic function of two random variables

Abbreviations

AM-AM	Amplitude dependent amplitude nonlinearity
AM-PM	Amplitude dependent Phase nonlinearity
BER	Bit error rate
BPNL	Bandpass nonlinearity
BPSK	Binary Phase Shift Keying
CCI	Cochannel Interference
MPSK	M-ary phase shift keying
MSK	Minimum shift keying
OQPSK	Offset Quadrature Phase shift keying
QPSK	Quadrature Phase Shift keying
SNR	Signal to noise ratio
TWT	Travelling wave tube

CHAPTER 1
INTRODUCTION

General

In recent years, digital transmission techniques have been gaining increased usage compared to analogue counterpart in satellite communication due to the ever-growing demand for data communications. The efficiency of a satellite system depends upon the modulation scheme used for signalling. In the current satellite systems, the digital modulation techniques are widely used compared to the analogue modulation schemes because of their superior bandwidth efficiency, high capacity, better reliability and flexible traffic handling ability. The growth of satellite communication technology has increased the requirement for accessing the satellite channels from a large number of low-cost earth stations rather than from a small number of expensive common carrier oriented earth terminals [Gould and Lum (1975), page 121]. In this multiple access environment digital modulation techniques are able to permit large and small users equal access to the satellite system.

The main advantages of digital transmission techniques are as follows: They provide low error rate and high fidelity through error detection and correction; they are less sensitive to the system and channel noise; and they

2

provide communication privacy, ease and efficiency in multiplexing and flexibility of digital hardware implementation. Bandwidth efficiency is readily obtained in digital modulation schemes by increasing the number of levels in multi-level modulation schemes. Digital modulation methods such as phase shift keying also have the advantage of relatively low susceptibility to interference. [Gould and Lum (1975), page 81].

There are two important aspects to be considered in selecting a particular modulation technique. These are the power limitation in the satellite channel and the signal to noise ratio improvement in the demodulation process. In this regard, the most effective digital methods are considered to be binary and quaternary phase shift keying techniques. The binary PSK provides higher resistance to interference but, there is possibility of doubling the information rate without expanding the bandwidth by employing Quaternary PSK.

1.2 Quadrature-carrier Modulation Techniques

The ultimate objective of most communication systems is to transmit the maximum amount of information, using a limited bandwidth with acceptable probability of error and complexity. This goal may be achieved by using spectrally efficient modulation schemes which exhibit

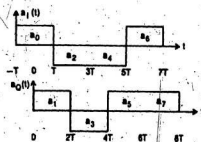
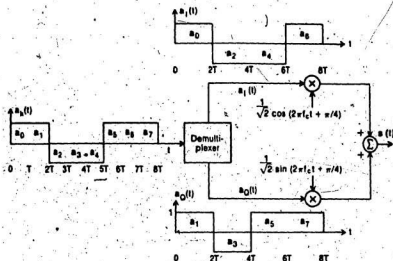
good error rate performance. The primary objective of spectrally efficient modulation is to maximize bandwidth efficiency which is defined as the ratio of the data rate to channel bandwidth. The secondary objective is to achieve this bandwidth efficiency at a prescribed average bit error rate with minimum expenditure of signal power. In the past decade, a class of constant envelope signals has received a great deal of attention because of its good error rate performance and simple detection schemes. These signalling schemes are known as quadrature - carrier modulation techniques.

In quadrature-carrier modulated signals, two carriers in phase quadrature, $\cos \omega_c t$ and $\sin \omega_c t$, are utilized for signalling. The data are independently modulated onto the two carriers. The detection of these signals can be accomplished by using simple receivers that provide the same error rate as in binary phase shift keying (BPSK) in an ideal additive white Gaussian noise channel. Therefore these modulation schemes are preferred to use when the RF spectrum is highly congested.

Among the quadrature carrier modulation methods Minimum shift keying (MSK) and Offset quadrature phase shift keying (OQPSK) have been preferred for use on a bandlimited nonlinear channels compared to the conventional Quadrature

phase shift keying due to the following reasons [Gronemeyer and McBride (1976)]. If either MSK signals or QPSK signals are bandlimited and then hard-limited, the degree of regeneration of the spectral sidelobes is less compared to QPSK. Also these techniques achieve the bit error rate performance of coherently detected BPSK on linear, infinite bandwidth, white Gaussian noise, perfect reference channels. Moreover, MSK and QPSK signals have carrier reference recovery features providing an advantage with respect to conventional QPSK. MSK can also be noncoherently detected when the received signal to noise ratio is adequate thus permitting an inexpensive demodulation.

A quadrature phase shift keying (QPSK) modulator is shown in Fig. 1.1 (A). A train of pulses a_K ($K=0,1,2,\dots$), of rate $\frac{1}{T}$ bits/sec arrives at the input of the demultiplexer as shown in the figure. The purpose of the demultiplexer is to split the incoming binary data stream into two Binary data streams each having a rate $\frac{1}{2T}$ bits/sec. This is done by directing even bits to inphase channel $a_I(t)$ and odd bits to quadrature phase channel $a_Q(t)$. These two binary streams modulate the inphase and quadrature carriers and the sum $s(t)$ is transmitted. The odd and even bit streams of pulse width $2T$ are synchronously aligned in QPSK so as to coincide their zero crossings as shown in the figure.



Offset QPSK modulation is obtained by offsetting the relative alignment of the inphase data stream $a_I(t)$ and quadrature bit stream $a_Q(t)$ by a single bit duration T . These waveforms are shown in Fig. 1.1(B).

Minimum shift keying (MSK) can be considered as a special case of offset QPSK with sinusoidal pulse weighting. Fig. 1.2(A) shows the waveform of the inphase data stream of MSK after sinusoidal pulse weighting. The modulated inphase carrier is obtained by multiplying this waveform by the inphase carrier $\cos 2\pi f_c t$. The resulting waveform is shown in Fig. 1.2(B). The sinusoidally shaped odd bit stream and the corresponding modulated carrier are shown in Figures 1.2(C) and 1.2(D). The transmitted signal $s(t)$ is obtained by summing the two modulated carriers as shown in Fig. 1.2(E).

These modulation schemes respond differently when they undergo bandlimiting and hard-limiting operations encountered in satellite communications. The difference in the behaviour can be explained by examining the phase changes in the respective carriers. Typical waveforms of MSK, OQPSK and QPSK are illustrated in Fig. 1.3. The phase transitions in MSK and OQPSK waveforms occur at every T seconds, but the conventional QPSK waveform has transitions only at $2T$ seconds as shown in the figure. In addition, MSK waveform has continuous phase as shown in Fig. 1.3. The offset QPSK and

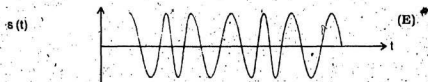
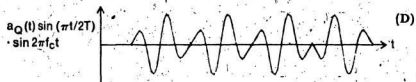
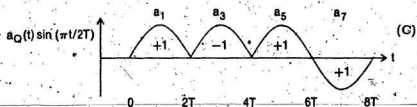
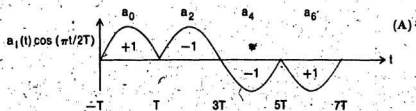


FIG. 1.2 MSK WAVEFORMS

QPSK waveforms have abrupt phase transitions as shown in Figure 1.3.

In offset QPSK phase change can be either $+90^\circ$ or -90° . But in the case of QPSK the phase transition of 180° is also possible. This possibility of 180° phase change in the QPSK modulation results in out of band radiation on the satellite downlink due to the limiting effects of the transponder. Since the maximum possible phase change is 90° in the offset QPSK, the out of band interference is much reduced [Pasupathy (1979)]. Further suppression of out of band interference is obtained in the case of MSK due to its continuous phase nature.

1.3 Cochannel Interference

The radio spectrum limitations have caused the necessity to share the same frequency band between satellite communication systems and terrestrial microwave networks. Also, the above limitation has necessitated the consideration and implementation of frequency-reuse techniques in satellite communication systems. The bandwidth efficiency of the satellite communication systems can be increased by utilizing the same carrier frequency more than once. Sharing the same frequency band with terrestrial networks and the frequency-reuse in satellite systems result in an increase in the level of cochannel interference.

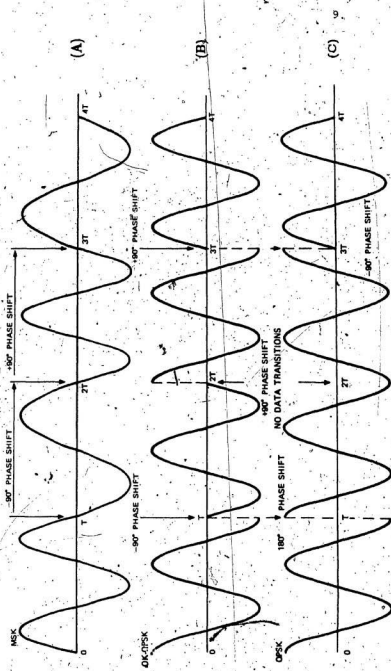


FIG. 1.3 TYPICAL WAVEFORMS FOR MSK, OFFSET QPSK AND QPSK

Cochannel interference is defined as an interference having the same frequency as that of the carrier. The source of this interference could be a cross polarized signal emanated from the same satellite, an intermodulation product, or a signal from a ground microwave link operating in the same band as the receive earth terminal.

The motivation for the study of cochannel interference in bandwidth efficient modulation techniques stems from the fact that the basic problem of spectral congestion is not solved but only lessened, by the use of these modulation schemes. Researchers have shown that bandwidth-efficient modulation techniques are sensitive to the cochannel interference [Cruz and Simpson (1981)]. Even with the best technology available today, cochannel interference, rather than thermal noise or intersymbol interference (ISI) due to the finite bandwidth of the filters in the system, is found to be the dominant cause of performance degradation [Kennedy and Shimbo (1981)]. At the same time, there has been only limited available analytical work for evaluating the effects of cochannel interference in a nonlinear satellite system.

1.4 Literature Review

In this section we briefly review the previous work

on the performance evaluation of quadrature-carrier modulated signals transmitted through satellite channels.

Forsey et al. (1978) have considered a satellite channel exhibiting AM-AM and AM-PM nonlinearities.. Independent narrowband Gaussian random processes were assumed on uplink and downlink. For this model they have derived an expression for the error probability of M-ary PSK signals. This error probability expression has been obtained in terms of an infinite series. They have also analysed the effect of TWT input power backoff on the error probability and shown that it is optimum to operate the TWT at the saturation region.

Mathews and Aghvami (1980) also have studied the performance of M-ary CPSK signals transmitted through a satellite channel. Their method is computationally superior to that obtained by Forsey et al. (1978) especially for multi-level ($M > 4$) CPSK signalling.

Mathews and Aghvami (1981) have also extended their previous work to include the case when cochannel interference is present along with the additive white Gaussian noise. They have derived exact expressions for the symbol error probability of binary and quaternary PSK transmissions.

The effect of CW tone interference and intersymbol interference (ISI) on the error rate performance of coherent MPSK signals transmitted through nonlinear satellite channels

has been analysed by Huang et al. (1981). In their model the additive Gaussian noise was assumed to be present only on the uplink. It has been shown that the performance degradation due to TWT input power backoff depends upon the slope of AM/PM characteristics.

Kennedy and Shimbo (1981) have analysed the effect of cochannel interference on QPSK signals transmitted through a nonlinear satellite channel. The effect of additive Gaussian noise has been considered on both the links but the effect of cochannel interference has been considered only in the uplink. They have pointed out the significance of the non-Gaussian nature of the interference.

Recently, expressions for the bit error rate of MSK and QPSK signals transmitted through a bandlimited nonlinear satellite channel have been derived by Ekanayake (1983). In his work, additive Gaussian noise was assumed to be present on both the links but the effect of intersymbol interference had been considered only in the uplink. It was shown that MSK is superior to QPSK under all signal and noise conditions.

1.5 Outline of the Thesis

The objective of the present work is to investigate the effect of cochannel interference on the error rate performance of MSK and QPSK signals transmitted through a

satellite channel. The satellite channel is assumed to exhibit both AM/AM and AM/PM nonlinearities. The additive white Gaussian noise is assumed to be present on both the uplink and the downlink but the cochannel interference is considered only in the uplink. The filters present in the system are assumed to be wideband so that the effect of intersymbol interference can be neglected.

In Chapter 2, a bit error rate expression for MSK signals is derived. An expression for the bit error probability of QPSK signals is obtained in Chapter 3. The numerical evaluation of the error rate performance of the two signalling techniques are presented in Chapter 4. In Chapter 5 conclusions are drawn and a few suggestions are made for further research.

CHAPTER 2

BIT ERROR RATE EXPRESSION FOR
MINIMUM SHIFT KEYING SIGNALS2.1 Introduction

This chapter deals with the development of an expression for the bit error probability of minimum shift keying (MSK) signals which have been transmitted through a nonlinear satellite channel in the presence of additive Gaussian noise and cochannel interference (CCI). The effect of additive Gaussian noise is considered in both the uplink and the downlink, but the effect of cochannel interference is considered only in the uplink.

Firstly, the effect of multiple cochannel interferers in the uplink is analysed and an expression for the bit error rate is obtained. The joint probability density function (PDF) of the inphase and quadrature baseband components is expressed in terms of the moments of the CCI random variables which are evaluated from their joint characteristic function. A power series expansion is employed to describe the joint characteristic function of the pair of random variables defining each cochannel interferer. Secondly, the case of the single cochannel interferer and Gaussian noise is analysed. An expression for the bit error probability for this case is derived from the conditional

joint probability density function without using any power series expansion.

Thirdly, an expression for the bit error rate in the absence of cochannel interference is obtained. Finally, by approximating the cochannel interference as Gaussian noise, a simple expression for the bit error probability is derived.

2.2 System Model

The communication system under consideration is illustrated in Fig. 2.1. The binary data a_k for $k=0,1,2,\dots$ are independent and identically distributed random variables which assume the values $+1$ and -1 with equal probability. The input binary stream arrives at a rate of $\frac{1}{T}$ bit/sec and is separated into two streams $a_1(t)$ and $a_0(t)$ consisting of even and odd bits respectively. The two pulse trains modulate the inphase and quadrature components of the carrier and the sum $S(t)$ is then transmitted. In the uplink, the signal is corrupted by the thermal noise and cochannel interference. Cochannel interference refers to the interference from a source having the same frequency as that of the carrier. The bandwidth of the transmitter filter, satellite filter and the receiver filter are assumed to be large enough to pass the signal without introducing intersymbol interference.

The signal is received by the satellite, filtered and then retransmitted to ground stations after power

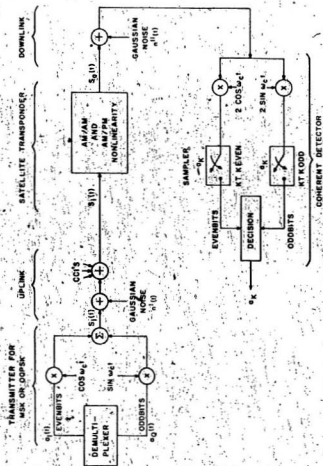


FIG. 2.1 MODEL FOR A SATELLITE COMMUNICATION SYSTEM

amplification using a TWT/amplifier. The TWT amplifier introduces bandpass nonlinearity which exhibits both AM/AM and AM/PM conversion effects. That is, for a sinusoidal input, the output is a sinusoid whose amplitude and phase are nonlinear functions of the input amplitude.

In the downlink the retransmitted signal is further corrupted by additive thermal noise to form the receiver input signal.

The receiver coherently demodulates the received signal $r(t)$ into inphase and quadrature baseband components. Then they are sampled at every $2T$ seconds and a decision is made as to whether the data bit in that bit period was +1 or -1.

2.3 Decision Circuit Input

The output of the transmitter, $s_1(t)$, which incorporates inphase and quadrature channels offset by one bit duration as in MSK signals, may be expressed as

$$s_1(t) = \sum_{k \text{ even}} a_k q(t-kT) \cos \omega_c t - \sum_{k \text{ odd}} a_k q(t-kT) \sin \omega_c t \quad (2.1)$$

The binary data a_k are assumed to be independent and identically distributed and take on the values +1 or -1 with equal probability.

The pulse shape $q(t)$ is defined for MSK as

$$q(t) = \begin{cases} A \cos(\pi t/2T) & -T < t < T \\ 0 & \text{elsewhere} \end{cases} \quad (2.2)$$

Since the data a_k are independent, in the following analysis it is sufficient to consider the signal during any data interval say $-T < t < T$.

In the uplink, signal $s_1(t)$ is corrupted by uplink additive Gaussian noise $n'(t)$ and cochannel interference $C(t)$.

The filtered uplink noise $n'(t)$ is represented as a narrowband process

$$n'(t) = n'_c(t) \cos \omega_c t - n'_s \sin \omega_c t \quad (2.3)$$

where n'_c and n'_s are independent, zero mean Gaussian processes of variance σ_u^2 . Eqn. (2.3) implies that the satellite bandpass filter centre frequency is the frequency of the signal carrier.

The cochannel interferers (CCI's) are assumed to be originated independently of each other, the transmitted signal $s_1(t)$ and the noise sources. In general, CCI may be the sum of the effects of $H(H=1,2,\dots)$ interferers each having the same carrier frequency as $s_1(t)$. The CCI during any data interval $-T < t < T$ may be represented as

$$C(t) = \sum_{k=1}^H A_k(t) [\cos \omega_c t \cos \phi_k - \sin \omega_c t \sin \phi_k] \quad (2.4)$$

The expressions $\sum_{k=1}^H A_k(t) \cos \phi_k$ and

$\sum_{k=1}^H A_k(t) \sin \phi_k$ are the inphase and quadrature components of the cochannel interference. A_k is the amplitude and ϕ_k is the random phase of the k^{th} interferer.

The signal entering the bandpass nonlinearity during the data interval $-T < t < T$ is the sum of $s_1(t)$, $n'(t)$ and $c(t)$ and may be written as

$$\begin{aligned} s_1(t) &= s_1(t) + n'(t) + c(t) \\ &= x(t) \cos \omega_c t - y(t) \sin \omega_c t \end{aligned} \quad (2.5)$$

By using trigonometric identities Eqn. (2.5) can be written as

$$s_1(t) = R(t) \cos[\omega_c t + \lambda(t)] \quad (2.6)$$

where

$$\begin{aligned} R(t) &= \sqrt{x^2(t) + y^2(t)} \\ \lambda(t) &= \tan^{-1}[y(t)/x(t)] \end{aligned} \quad (2.7)$$

$$x(t) = a_0 q(t) + \sum_{k=1}^H A_k(t) \cos \phi_k + n'_c$$

$$y(t) = a_{-1} q(t+T) + a_1 q(t-T) + \sum_{k=1}^H A_k(t) \sin \phi_k + n'_s$$

In Eqn. (2.7), $R(t)$ and $\lambda(t)$ are the amplitude and phase angle of the signal $s_1(t)$; $x(t)$ and $y(t)$ are the quadrature components of $s_1(t)$; $a_0 q(t)$ is the inphase signal component; and $a_{-1} q(t+T)$, $a_1 q(t-T)$ are the quadrature signal components during the data interval $-T < t < T$. On amplification of the signal $s_1(t)$, the TWT amplifier in the satellite transponder

will introduce AM/AM and AM/PM nonlinearities to it.

The output from the BPNL, $s_0(t)$, is

$$s_0(t) = f(R) \cos[\omega_c t + \lambda(t) + \phi(R)] \quad (2.8)$$

where $f(\cdot)$ and $\phi(\cdot)$ denote the AM/AM and AM/PM conversions of the Bandpass nonlinearity, respectively.

In the downlink the signal $s_0(t)$ is again corrupted by the additive Gaussian noise, $n''(t)$, whose quadrature components are given as n_c'' and n_s'' . The narrowband downlink noise $n''(t)$ is

$$n''(t) = n_c''(t) \cos \omega_c t - n_s''(t) \sin \omega_c t \quad (2.9)$$

Both n_c'' and n_s'' are zero mean Gaussian processes of variance σ_d^2 . Therefore the received signal can be written as

$$\begin{aligned} r(t) = s_0(t) + n''(t) = f(R) \cos[\omega_c t + \lambda(t) + \phi(R)] \\ + n_c''(t) \cos \omega_c t - n_s''(t) \sin \omega_c t \end{aligned} \quad (2.10)$$

The receiver demodulates the received signal $r(t)$ into inphase and quadrature baseband components by using a coherent reference carrier. The inphase baseband waveform is sampled at $t=t_0+kT$ for even values of k and then a decision is made on the data a_k for these values of k . Similarly the quadrature baseband waveform is sampled at $t=t_0+kT$ for odd values of k and a decision is made on the data a_k for these values of k . The time t_0 is the instant at which the pulse $q(t)$ attains its peak. In this case the inphase baseband component is sampled at $t=0$ during the data interval $-T < t < T$.

and a decision is made to determine whether a_0 is +1 or -1. The value of the quadrature baseband component will be zero at the sampling instant $t=0$ due to the half sinusoidal pulse weighting. The value of the inphase baseband sample at $t=t_0$, is

$$x'(t_0) = f(R) \cos[\lambda(t_0) + \phi(R)] + n_c'(t_0) \quad (2.11)$$

Since a_0 assumes the value +1 or -1 with equal probability, by evaluating the error in the decision when $a_0 = +1$ the probability of error can be obtained.

2.4 Probability of Bit Error

2.4.1 Conditional Probability of Bit Error

Initially, it is assumed that the quadrature components n_c' and n_s' of the uplink additive Gaussian noise and the cochannel interference are known, and the probability of error of the inphase baseband bit decision conditioned on n_c' , n_s' and the CCI random variables α and β , is determined. The problem then reduces to the determination of the probability of error of the inphase baseband bit decision when an additive Gaussian noise is added in the downlink to a sinusoid of known amplitude and phase. The probability of bit error conditioned on n_c' , n_s' and CCI random variables may be obtained as follows.

By omitting the time variable t_0 in Eqn. (2.11) the value of the inphase baseband component is expressed as

$$x' = f(R) \cos(\theta) + n_c^n \quad (2.12)$$

where $\theta = \lambda(t_0) + \phi(R)$. Also

$$n_c^n = x' - f(R) \cos \theta \quad (2.13)$$

The probability of bit error P_e' conditioned on uplink random noise and interference is written as

$$P_e' = \frac{1}{2} \int_{-\infty}^0 p(x'/+1) dx' + \frac{1}{2} \int_0^{\infty} p(x'/-1) dx' \quad (2.14)$$

Since $a_0 = \pm 1$, with equal probability

$$P_e' = \int_{-\infty}^0 p(x'/+1) dx' \quad (2.15)$$

The term $f(R) \cos \theta$ is known and n_c^n is a Gaussian random variable having zero mean and variance σ_d^2 . Hence

$$p(x') = \frac{1}{\sqrt{2\pi} \sigma_d^2} e^{-(x' - f(R) \cos \theta)^2 / 2\sigma_d^2} \quad (2.16)$$

By substituting Eqn. (2.16) in Eqn. (2.15) P_e' is obtained as

$$P_e' = \int_{-\infty}^0 \frac{1}{\sqrt{2\pi} \sigma_d^2} e^{-(x' - f(R) \cos \theta)^2 / 2\sigma_d^2} dx' \quad (2.17)$$

The error function $\text{erf}(v)$ is defined as

$$\text{erf}(v) = \frac{2}{\sqrt{\pi}} \int_0^v e^{-u^2} du \quad (2.18)$$

and the complementary error function $\text{erfc}(v)$ is defined as

$$\operatorname{erfc}(v) = 1 - \operatorname{erf}(v) = \frac{2}{\sqrt{\pi}} \int_v^{\infty} e^{-u^2} du \quad (2.19)$$

Substituting $u = \frac{x' - f(R) \cos \theta}{\sqrt{2} \sigma_d}$ in Eqn. (2.17), P_e' can be written as,

$$P_e' = \frac{1}{2} \frac{2}{\sqrt{\pi}} \int \frac{f(R) \cos \theta}{\sqrt{2} \sigma_d} e^{-u^2} du \quad (2.20)$$

$$P_e' = \frac{1}{2} \operatorname{erfc} \left[\frac{f(R) \cos \theta}{\sqrt{2} \sigma_d} \right] = \frac{1}{2} \left[1 - \operatorname{erf} \left[\frac{f(R) \cos \theta}{\sqrt{2} \sigma_d} \right] \right] \quad (2.21)$$

where $\theta = \lambda(t_0) + \phi(R)$

σ_d = variance of the downlink Gaussian noise components

The conditioning may be removed by taking the expectation of P_e' over n_c' , n_s' and CCI random variables α and β .

Alternatively, the conditioning on uplink random variables can be removed by taking the expectation of P_e' over the random variables x and y which are defined in Eqn. (2.7).

Firstly we have to evaluate the joint probability density function (PDF) of the random variables x and y to obtain the expectation of P_e' . The method illustrated by Ekanayake (1983) is used to obtain the joint PDF of x and y .

2.4.2 Joint Probability Density Function $p(x,y)$

The evaluation of the joint PDF $p(x,y)$ can be done as follows. From Eqn. (2.7), the random variables x and y

can be written as

$$\begin{aligned}x &= a_0 q_0 + \alpha + n'_c \\y &= \beta + n'_s\end{aligned}\quad (2.22)$$

where

$$\alpha = \sum_{k=1}^H A_k(t) \cos \phi_k$$

and

$$\beta = \sum_{k=1}^H A_k(t) \sin \phi_k$$

are the cochannel interference due to $H(H=1,2,\dots)$ interferers in the inphase and quadrature channels respectively. Since n'_c and n'_s are Gaussian random variables, the joint PDF of x and y conditional on the cochannel interference random variables α and β is obtained as

$$p(x,y/\alpha,\beta) = \frac{1}{2\pi \sigma_u^2} \exp\left[-\left(\frac{x-q_0-\alpha}{\sqrt{2} \sigma_u}\right)^2\right] \exp\left[-\left(\frac{y-\beta}{\sqrt{2} \sigma_u}\right)^2\right] \quad (2.23)$$

where σ_u^2 is the uplink noise power.

The generating function $g(x,z)$ is defined by Abramowitz and Stegun (1972) as

$$g(x,z) = e^{2xz-z^2} = \sum_{n=0}^{\infty} \frac{1}{n!} H_n(x) z^n \quad (2.24)$$

From Eqn. (2.23) we can write

$$\exp\left[-\left(\frac{x-q_0-\alpha}{\sqrt{2} \sigma_u}\right)^2\right] = \exp\left[-\left(\frac{x-q_0}{\sqrt{2} \sigma_u}\right)^2\right] \exp\left[-\frac{2(x-q_0)\alpha-\alpha^2}{(\sqrt{2} \sigma_u)^2}\right] \quad (2.25)$$

Using the definition of $g(x, z)$ in equation (2.24) we note that

$$\begin{aligned}
 g\left(\frac{x-q_0}{\sqrt{2} \sigma_u}, \frac{a}{\sqrt{2} \sigma_u}\right) &= \exp\left[-\frac{2(x-q_0)a-a^2}{(\sqrt{2} \sigma_u)^2}\right] \\
 &= \sum_{l=0}^{\infty} \frac{1}{l!} H_l\left(\frac{x-q_0}{\sqrt{2} \sigma_u}\right) \left(\frac{a}{\sqrt{2} \sigma_u}\right)^l.
 \end{aligned} \quad (2.26)$$

From Eqn. (2.23) we can write

$$\exp\left[-\left(\frac{y-\beta}{\sqrt{2} \sigma_u}\right)^2\right] = \exp\left[-\left(\frac{y}{\sqrt{2} \sigma_u}\right)^2\right] \exp\left[\frac{2y\beta-\beta^2}{(\sqrt{2} \sigma_u)^2}\right] \quad (2.27)$$

Using the definition of $g(x, z)$ in equation (2.24), we note that

$$\begin{aligned}
 g\left(\frac{y}{\sqrt{2} \sigma_u}, \frac{\beta}{\sqrt{2} \sigma_u}\right) &= \exp\left[\frac{2y\beta-\beta^2}{(\sqrt{2} \sigma_u)^2}\right] \\
 &= \sum_{m=0}^{\infty} \frac{1}{m!} H_m\left(\frac{y}{\sqrt{2} \sigma_u}\right) \left(\frac{\beta}{\sqrt{2} \sigma_u}\right)^m.
 \end{aligned} \quad (2.28)$$

By substituting Eqn. (2.26) in Eqn. (2.25) we can write

$$\begin{aligned}
 \exp\left[-\left(\frac{x-q_0-a}{\sqrt{2} \sigma_u}\right)^2\right] &= \exp\left[-\left(\frac{x-q_0}{\sqrt{2} \sigma_u}\right)^2\right] \sum_{l=0}^{\infty} \frac{1}{l!} H_l\left(\frac{x-q_0}{\sqrt{2} \sigma_u}\right) \\
 &\quad \times \left(\frac{a}{\sqrt{2} \sigma_u}\right)^l
 \end{aligned} \quad (2.29)$$

and by substituting Eqn. (2.28) in Eqn. (2.27) we can write

$$\exp[-(\frac{y-\beta}{\sqrt{2} \sigma_u})^2] = \exp[-(\frac{y}{\sqrt{2} \sigma_u})^2] \sum_{m=0}^{\infty} \frac{1}{m!} H_m(\frac{y}{\sqrt{2} \sigma_u}) \times (\frac{\beta}{\sqrt{2} \sigma_u})^m \quad (2.30)$$

Then substituting Eqn. (2.29) and Eqn. (2.30) in Eqn. (2.23)

$p(x, y/a, \beta)$ is obtained as

$$p(x, y/a, \beta) = \frac{1}{2\pi \sigma_u^2} \exp[-(\frac{x-q_0}{\sqrt{2} \sigma_u})^2] \exp[-(\frac{y}{\sqrt{2} \sigma_u})^2] \times \sum_{l,m} \left(\frac{1}{\sqrt{2} \sigma_u}\right)^{l+m} \frac{a \cdot \beta^m}{l! m!} \times H_l\left(\frac{x-q_0}{\sqrt{2} \sigma_u}\right) H_m\left(\frac{y}{\sqrt{2} \sigma_u}\right) \quad (2.31)$$

where $H_n(\cdot)$ denotes Hermite polynomials, $n!$ denotes the

factorial of n and the notation $\sum_{l,m}$ signifies the summation

over all positive integer values of l and m . The joint PDF

$p(x, y)$ can be obtained by taking the expected value of the conditional PDF $p(x, y/a, \beta)$ over the random variables a and β .

Therefore the PDF $p(x, y)$ is expressed in terms of the moments of the CCI random variables as

$$p(x, y) = \frac{1}{2\pi \sigma_u^2} \exp[-(\frac{x-q_0}{\sqrt{2} \sigma_u})^2] \exp[-(\frac{y}{\sqrt{2} \sigma_u})^2] \times \sum_{l,m} \left(\frac{1}{\sqrt{2} \sigma_u}\right)^{l+m} \frac{E[a^l \beta^m]}{l! m!} \times H_l\left(\frac{x-q_0}{\sqrt{2} \sigma_u}\right) H_m\left(\frac{y}{\sqrt{2} \sigma_u}\right) \quad (2.32)$$

Next, we have to evaluate the joint characteristic function of the random variables α and β in order to obtain the moments of the CCI random variables.

2.4.3 Evaluation of the Moments of the Random Variables α , β

The joint characteristic function of the random variables α and β is given by

$$\phi(u, v) = E[\exp[j(\alpha u + \beta v)]] \quad (2.33)$$

The characteristic function, which always exists, can be used to generate the moments of the random variables. The cochannel interference from Eqn. (2.4) can be written as

$$C(t) = \sum_{k=1}^H A_k [\cos \omega_c t \cos \phi_k + \sin \omega_c t \sin \phi_k] \quad (2.34)$$

First, assume that the cochannel interferers are concentrated in a single interferer. Then the cochannel interference can be written as

$$C(t) = A [\cos \omega_c t \cos \phi - \sin \omega_c t \sin \phi] \quad (2.35)$$

where A is the amplitude of the CCI which is a constant, and ϕ is the random phase of the interfering signal, this phase being assumed to be independent of the other random variables and uniformly distributed between 0 and 2π . We may define

$$\begin{aligned} \alpha &= A \cos \phi \\ \beta &= A \sin \phi \end{aligned} \quad (2.36)$$

where a and b are the inphase and quadrature components of the CCI. Therefore, the joint characteristic function of the random variables a and b is written as

$$\phi(u, v) = E[\exp\{j(uA \cos \phi + vA \sin \phi)\}] \quad (2.37)$$

Since the amplitude A is a constant and the random phase ϕ is uniformly distributed between 0 and 2π , the joint characteristic function $\phi(u, v)$ can be written as

$$\phi(u, v) = \frac{1}{2\pi} \int_0^{2\pi} \exp\{j[u \cos \phi + v \sin \phi]\} d\phi \quad (2.38)$$

The above equation can be rewritten as

$$\phi(u, v) = \frac{1}{2\pi} \int_0^{2\pi} \exp\{jz \cos(\phi - \lambda)\} d\phi \quad (2.39)$$

where

$$z = \sqrt{(uA)^2 + (vA)^2} \quad (2.40)$$

$$\lambda = \tan^{-1}\left(\frac{v}{u}\right)$$

The parameter λ is a constant and ϕ is uniformly distributed between 0 and 2π . By substituting $\theta = \phi - \lambda$ in Eqn. (2.39) we can write

$$\begin{aligned} \phi(u, v) &= \frac{1}{2\pi} \int_{-\lambda}^{2\pi-\lambda} \exp\{jz \cos \theta\} d\theta \\ &= \frac{1}{\pi} \int_0^{\pi} \exp\{jz \cos \theta\} d\theta \\ &= J_0(z) = J_0(\sqrt{u^2 + v^2}) \end{aligned} \quad (2.41)$$

where

$$J_n(z) = \frac{1}{\pi} \int_0^\pi \exp(jz \cos \theta) \cos(n\theta) d\theta \quad (2.42)$$

is the Bessel function of the first kind of order n . If there are H independent interferers with amplitude A_k ($k=1, 2, \dots, H$) and random phase ϕ_k which is uniformly distributed between 0 and 2π then from Eqn. (2.34) we may write

$$\begin{aligned} \alpha_k &= \sum_{k=1}^H A_k \cos \phi_k \\ \beta_k &= \sum_{k=1}^H A_k \sin \phi_k \end{aligned} \quad (2.43)$$

where α_k and β_k are the inphase and quadrature components of the CCI. Since each cochannel interferers are independent and identically distributed, the joint characteristic function is the product of the characteristic functions of each individual interferer. Therefore, the joint characteristic function of H independent interferers can be written as

$$\begin{aligned} \phi(u, v) &= \phi(u_1, v_1) \phi(u_2, v_2) \dots \phi(u_H, v_H) \\ &= \prod_{k=1}^H \phi(u_k, v_k) \end{aligned} \quad (2.44)$$

By using Eqn. (2.41) the above equation can be written as

$$\phi(u, v) = \prod_{k=1}^H J_0(A_k \sqrt{u^2 + v^2}) \quad (2.45)$$

As shown in Appendix A, the characteristic function $\phi(u,v)$ can be expanded in a power series as

$$\phi(u,v) = \sum_{l,m} b_{l,m} u^l v^m \quad (2.46)$$

l, m even

We can now obtain the moment of order $l+m$ by

$$\begin{aligned} \frac{\partial^{l+m}}{\partial u^l \partial v^m} \phi_{\alpha, \beta}(u,v) \bigg|_{u=0, v=0} &= E(\alpha^l \beta^m) = \mu_{l,m} \\ &= \frac{\partial^{l+m}}{\partial u^l \partial v^m} \left[\sum_{l,m} b_{l,m} u^l v^m \right] \bigg|_{u=0, v=0} \\ &= (-1)^{-(l+m)/2} l! m! b_{l,m} \end{aligned} \quad (2.47)$$

Therefore the moments of the CCI random variables α and β are obtained as

$$E[\alpha^l \beta^m] = (-1)^{(l+m)/2} l! m! b_{l,m} \quad (2.48)$$

The required expression for the joint PDF $p(x,y)$ can be obtained by substituting Eqn. (2.48) in Eqn. (2.32)

2.4.4 Expression for Bit Error Probability

The expression for the bit error rate (BER) can be obtained by evaluating the expectation of P_e using the joint PDF $p(x,y)$ as

$$P_e = \int_{-\infty}^{\infty} \int_{-\infty}^{\infty} P_e'(x,y) p(x,y) dx dy \quad (2.49)$$

Therefore, by substituting equations (2.21), (2.32) and (2.48) in Eqn. (2.49), the Bit error probability is expressed

as

$$\begin{aligned}
 P_e = & \frac{1}{2} - \frac{1}{4\pi \sigma_u^2} \int_{-\infty}^{\infty} \int_{-\infty}^{\infty} b_{l,m} (-1)^{(l+m)/2} \left(\frac{y}{\sqrt{2} \sigma_u} \right)^{l+m} \\
 & \times \int_{-\infty}^{\infty} \int_{-\infty}^{\infty} \operatorname{erf} \left[\frac{f(R) \cos \theta}{\sqrt{2} \sigma_d} \right] H_l \left(\frac{x}{\sqrt{2} \sigma_u} - \rho_u \right) H_m \left(\frac{y}{\sqrt{2} \sigma_u} \right) \\
 & \times \exp \left[- \left(\frac{x}{\sqrt{2} \sigma_u} - \rho_u \right)^2 \right] \exp \left[- \left(\frac{y}{\sqrt{2} \sigma_u} \right)^2 \right] dx dy
 \end{aligned} \quad (2.50)$$

The parameter ρ_u , which is the uplink carrier power to noise power ratio (CNR), is given as

$$\rho_u^2 = \frac{q_0^2}{2\sigma_u^2} \quad (2.51)$$

The downlink carrier power to noise power ratio (CNR) is defined as

$$\rho_d^2 = \frac{f^2(R)}{2\sigma_d^2} \quad (2.52)$$

where $f^2(R)/2$ is the average value of the downlink carrier power. The BER expression given in Eqn. (2.50) can be simplified by changing the variables x and y to r and s using the relations:

$$\begin{aligned}
 r &= \frac{x - q_0}{\sqrt{2} \sigma_u} \quad \text{and} \\
 s &= \frac{y}{\sqrt{2} \sigma_u}
 \end{aligned} \quad (2.53)$$

and can be written as

$$P_e = \frac{1}{2} - \frac{1}{2\pi} \int_{-\infty}^{\infty} \int_{-\infty}^{\infty} (-1)^{(l+m)/2} (\rho_u)^{l+m} \frac{b_{l,m}}{(q_0)^{l+m}} \\ \times \int_{-\infty}^{\infty} \int_{-\infty}^{\infty} \operatorname{erf}[\rho_d \frac{f(R) \cos \theta}{\sqrt{f^2(R)}}] \\ \times H_l(r) H_m(s) \exp[-(r^2 + s^2)] dr ds$$

where

$$R^2 = [q_0^2 (r + \rho_u)^2 + (q_0 s)^2] / \rho_u^2 \quad (2.55) \\ \theta = \phi(R) + \tan^{-1} \left(\frac{s}{r + \rho_u} \right)$$

Also, $b_{l,m}$ denotes the coefficients of the power series expansion of the joint characteristic function of the CCI random variables α and β .

The term q_0 denotes the magnitude of the sample at the sampling instant which is taken as unity. The AM/AM and AM/PM nonlinearities, $f(R)$ and $\phi(R)$ respectively, are determined from the TWT Characteristics which shall be illustrated in Chapter 4.

2.5 Probability of Bit Error With Single Cochannel Interferer

In this section we consider the derivation of an alternative expression for the bit error probability when there is only one cochannel interferer present in the uplink.

To this end joint PDF of x and y conditional on the CCI random variable α and β from Eqn. (2.23) is rewritten as

$$p(x, y/\alpha, \beta) = \frac{1}{2\pi \sigma_u^2} \exp\left[-\left(\frac{x - q_0 - \alpha}{\sqrt{2} \sigma_u}\right)^2\right] \exp\left[-\left(\frac{y - \beta}{\sqrt{2} \sigma_u}\right)^2\right] \quad (2.56)$$

where

$$\begin{aligned} \alpha &= A \cos \phi \\ \beta &= A \sin \phi \end{aligned} \quad (2.57)$$

Also, A is the amplitude and ϕ is the random phase of the CCI which is uniformly distributed between 0 and 2π . Then the PDF $p(x, y)$ is

$$p(x, y) = \int_0^{2\pi} p(x, y/\alpha, \beta) p(\phi) d\phi \quad (2.58)$$

Therefore, by combining Eqn. (2.56) and Eqn. (2.58), joint PDF $p(x, y)$ is written as

$$\begin{aligned} p(x, y) &= \frac{1}{2\pi} \int_0^{2\pi} \frac{1}{2\pi \sigma_u^2} \exp\left[-\left(\frac{x - q_0 - A \cos \phi}{\sqrt{2} \sigma_u}\right)^2\right] \\ &\quad \times \exp\left[-\left(\frac{y - A \sin \phi}{\sqrt{2} \sigma_u}\right)^2\right] d\phi \\ &= \frac{1}{2\pi \sigma_u^2} \exp\left[-\left(\frac{x - q_0}{\sqrt{2} \sigma_u}\right)^2\right] \exp\left[-\left(\frac{y}{\sqrt{2} \sigma_u}\right)^2\right] \\ &\quad \times \exp\left[-\left(\frac{A}{\sqrt{2} \sigma_u}\right)^2\right] \frac{1}{2\pi} \\ &\quad \times \int_0^{2\pi} \exp\left[\frac{A[2(x - q_0) \cos \phi + 2y \sin \phi]}{2\sigma_u^2}\right] d\phi \end{aligned} \quad (2.59)$$

The integration with respect to ϕ can be carried out readily and the joint PDF $p(x,y)$ is obtained as

$$p(x,y) = \frac{1}{2\pi\sigma_u^2} \exp\left[-\left(\frac{x-q_0}{\sqrt{2}\sigma_u}\right)^2\right] \exp\left[-\left(\frac{y}{\sqrt{2}\sigma_u}\right)^2\right] \\ \times \exp\left[-\left(\frac{A}{\sqrt{2}\sigma_u}\right)^2\right] I_0(x) \quad (2.60)$$

where

$$x = \frac{\sqrt{2}}{\sigma_u} A \sqrt{\left(\frac{x-q_0}{\sqrt{2}\sigma_u}\right)^2 + \left(\frac{y}{\sqrt{2}\sigma_u}\right)^2} \quad (2.61)$$

The expression for the bit error probability in the presence of single cochannel interferer and additive Gaussian noise may be obtained by evaluating the expectation of P_e given in Eqn. (2.21) using the joint PDF $p(x,y)$ given in Eqn. (2.60). Therefore, the bit error probability is expressed as

$$P_e = \frac{1}{2} - \frac{1}{4\pi\sigma_u^2} \exp\left[-\left(\frac{A}{\sqrt{2}\sigma_u}\right)^2\right] \int_{-\infty}^{\infty} \int_{-\infty}^{\infty} \operatorname{erf}\left[\frac{f(R) \cos \theta}{\sqrt{2}\sigma_d}\right] \\ \times I_0\left[\frac{\sqrt{2}A}{\sigma_u} \sqrt{\left(\frac{x-q_0}{\sqrt{2}\sigma_u}\right)^2 + \left(\frac{y}{\sqrt{2}\sigma_u}\right)^2}\right] \\ \times \exp\left[-\left(\frac{x}{\sqrt{2}\sigma_u} - \rho_u\right)^2\right] \exp\left[-\left(\frac{y}{\sqrt{2}\sigma_u}\right)^2\right] dx dy \quad (2.62)$$

The above expression can be simplified by changing the variables x and y to r and s using the relations given in Eqn. (2.53). Then the probability of bit error P_e can be written as

$$P_e = \frac{1}{2} - \frac{1}{2\pi} \exp\left[-\left(\frac{p_u A}{q_0}\right)^2\right] \int_{-\infty}^{\infty} \int_{-\infty}^{\infty} \operatorname{erf}\left[\rho_d \frac{f(R) \cos \theta}{\sqrt{f^2(R)}}\right] \\ \times I_0\left[\frac{2p_u A}{q_0} \sqrt{r^2 + s^2}\right] \exp[-(r^2 + s^2)] dr ds \quad (2.63)$$

where R and θ are defined in Eqn. (2.55)

2.6 Probability of Bit Error in the Absence of Cochannel Interference

In the absence of cochannel interference the joint PDF $p(x, y)$ is obtained from Eqn. (2.23) as

$$p(x, y) = \frac{1}{2\pi \sigma_u^2} \exp\left[-\left(\frac{x - q_0}{\sqrt{2} \sigma_u}\right)^2\right] \exp\left[-\left(\frac{y}{\sqrt{2} \sigma_u}\right)^2\right] \quad (2.64)$$

The expression for bit error probability in Gaussian case is obtained by combining Eqn. (2.21) and Eqn. (2.64) as

$$P_e = \frac{1}{2} - \frac{1}{4\pi \sigma_u^2} \int_{-\infty}^{\infty} \int_{-\infty}^{\infty} \operatorname{erf}\left[\frac{f(R) \cos \theta}{\sqrt{2} \sigma_d}\right] \\ \times \exp\left[-\left(\frac{x}{\sqrt{2} \sigma_u} - \rho_u\right)^2\right] \exp\left[-\left(\frac{y}{\sqrt{2} \sigma_u}\right)^2\right] dx dy \quad (2.65)$$

The above expression can be expressed in simplified form by changing the variables x and y to r and s using the relations given in Eqn. (2.53).

The simplified expression for the BER is

$$P_e = \frac{1}{2} - \frac{1}{2\pi} \int_{-\infty}^{\infty} \int_{-\infty}^{\infty} \text{erf}[\rho_d \frac{f(R) \cos \theta}{\sqrt{f^2(R)}}] \times \exp[-(r^2 + s^2)] dr ds \quad (2.66)$$

where R and θ are defined in Eqn. (2.55).

For $k = m = 0$, the BER expression given in Eqn. (2.54) will reduce to the Gaussian case which is given in Eqn. (2.66). In the absence of cochannel interference, substituting the amplitude $A=0$ in Eqn. (2.63) also will provide the BER expression given in Equation (2.66).

2.7 Gaussian Approximation

In this section we derive an expression for the bit error probability in the presence of cochannel interference and Gaussian noise which can be computed more efficiently than the BER expression derived in Section 2.4.

By approximating the cochannel interference as a Gaussian noise source, the total noise power σ^2 can be obtained as [Shimbo and Fang (1973)]

$$\sigma^2 = \sigma_u^2 + \sigma_k^2 \quad (2.67)$$

where σ^2 is the sum of the Gaussian noise power σ_u^2 and the cochannel interference power σ_k^2 .

The joint characteristic function of the random variables α and β for $H(H=1,2,\dots,\infty)$ interferers which is

defined in Eqn. (2.45), may be approximated by an exponential expression as suggested by Jain (1972) and written as,

$$\begin{aligned}\phi(u,v) &= \prod_{k=1}^H j_0(\lambda_k \sqrt{u^2 + v^2}) = \exp\left[-\frac{1}{2} \sigma_k^2 (u^2 + v^2)\right] \\ &= \exp\left[-\frac{1}{2} \sigma_k^2 u^2\right] \exp\left[-\frac{1}{2} \sigma_k^2 v^2\right]\end{aligned}\quad (2.68)$$

where

$$\sigma_k^2 = \frac{1}{2} \sum_{k=1}^H \lambda_k^2 \quad (2.69)$$

The probability density function of x is defined as

$$p(x) = \frac{1}{2\pi} \int \phi(u) e^{-iux} du \quad (2.70)$$

By using the above definition, the joint PDF of x and y is obtained from the joint characteristic function which is approximated by the exponential expression in Eqn. (2.68) as

$$p(x,y) = \frac{1}{\sqrt{2\pi} \sigma^2} \exp\left[-\frac{x^2}{2\sigma^2}\right] \frac{1}{\sqrt{2\pi} \sigma^2} \exp\left[-\frac{y^2}{2\sigma^2}\right] \quad (2.71)$$

Therefore the joint PDF of x and y may be obtained from Eqn. (2.23) by assuming α and β as zero and can be written as

$$p(x,y) = \frac{1}{2\pi \sigma^2} \exp\left[-\frac{(x-q_0)^2}{2\sigma^2}\right] \exp\left[-\frac{y^2}{2\sigma^2}\right] \quad (2.72)$$

The above expression is the same as the joint PDF $p(x,y)$ in the absence of cochannel interference which is given in

Eqn. (2.64), except for the difference in the noise variance

σ^2 .

The expression for bit error probability may thus be recalled from Eqn. (2.65) as

$$P_e = \frac{1}{2} - \frac{1}{4\pi\sigma^2} \int_{-\infty}^{\infty} \int_{-\infty}^{\infty} \operatorname{erf}\left[\frac{f(R) \cos \theta}{\sqrt{2}\sigma_d}\right] \times \exp\left[-\left(\frac{x}{\sqrt{2}\sigma} - \rho_u\right)^2\right] \exp\left[-\left(\frac{y}{\sqrt{2}\sigma}\right)^2\right] dx dy \quad (2.73)$$

In the above expression the noise power σ^2 is given in Eqn. (2.67). The expression given in Eqn. (2.73) is simplified by changing the variables x and y to r and s using the relations given in Eqn. (2.53). Therefore, the BER expression is recalled from Eqn. (2.66) and written as

$$P_e = \frac{1}{2} - \frac{1}{2\pi} \int_{-\infty}^{\infty} \int_{-\infty}^{\infty} \operatorname{erf}\left[\rho_d \frac{f(R) \cos \theta}{\sqrt{f^2 R}}\right] \times \exp[-(\tau^2 + s^2)] dr ds \quad (2.74)$$

where

$$\begin{aligned} \theta &= \phi(R) + \tan^{-1} \left[\frac{\sqrt{2} s \sigma}{\sqrt{2} \tau \sigma + q_0} \right] \\ R^2 &= (\sqrt{2} \tau \sigma + q_0)^2 + (\sqrt{2} s \sigma)^2 \\ \sigma_u^2 &= \sigma_u^2 + \sigma_k^2 = \frac{q_0^2}{2\rho_u} + \frac{1}{2} \sum_{k=1}^H A_k^2 \end{aligned} \quad (2.75)$$

CHAPTER 3

BIT ERROR RATE EXPRESSION FOR OFFSETQUADRATURE PHASE SHIFT KEYING SIGNALS3.1 Introduction

In this chapter we consider the bit error probability evaluation of offset quadrature phase shift keying (OQPSK) signals which have been transmitted through nonlinear satellite channels in the presence of additive Gaussian noise and cochannel interference (CCI). The main steps of the analytical procedure are similar to that followed in Chapter 2, but certain modifications are required for the reason outlined below.

In the case of MSK signals, due to its half sinusoidal pulse weighting, the quadrature baseband component has a zero crossing at the sampling instant of the inphase baseband component. Therefore there is no interference from the quadrature baseband component. But in the case of OQPSK signals, the quadrature baseband component has no zero crossing at the sampling instant of the inphase baseband component due to its rectangular pulse weighting. Therefore the interference from the quadrature baseband component has to be taken into account in analyzing the bit error rate of OQPSK signals.

First we consider the case when the signal is distorted by multiple cochannel interferers and then the case when the signal is distorted by single cochannel interferer. For each case we obtain the bit error rate expressions which are different from each other. The expression for the probability of error in the absence of cochannel interference is also obtained.

3.2 Decision Circuit Input

The model for the QPSK signalling satellite system is the same as for the MSK signalling satellite system which was shown in Fig. 2.1. Thus the output of the transmitter, $S_1(t)$, may be reproduced from Eqn. (2.1) as

$$S_1(t) = \begin{cases} I \sum_{k \text{ even}} a_k q(t - kT) \cos \omega_c t \\ -I \sum_{k \text{ odd}} q(t - kT) \sin \omega_c t \end{cases} \quad (3.1)$$

The modulating pulse stream $q(t)$, in the case of offset QPSK, which is having rectangular shape may be defined as

$$q(t) = \begin{cases} A/2 & -Tt < T \\ 0 & \text{elsewhere} \end{cases} \quad (3.2)$$

In the uplink, the signal $S_1(t)$ is corrupted by the narrowband Gaussian noise $n(t)$ given in Eqn. (2.3) and cochannel interference $c(t)$, given in Eqn. (2.4). The input signal to the TWT amplifier is further corrupted during the process of amplification due to the AM/AM and AM/PM

nonlinearities.

In the downlink, the output signal from the TWT amplifier is again corrupted by a narrowband Gaussian noise process. Thus the expression for the received signal $r(t)$ is same as in the case of MSK signals which was given in Eqn. (2.10) and may be reproduced as

$$r(t) = f(R) \cos[\omega_c t + \lambda(t) + \phi(R)] + n_c''(t) \cos \omega_c t - n_s'' \sin \omega_c t \quad (3.3)$$

where $\lambda(t)$ is defined in Eqn. (2.7) and where $f(R)$ and $\phi(R)$ are the AM/AM and AM/PM nonlinearities, respectively. After demodulating the received signal into inphase and quadrature baseband components, a sample is taken from the inphase baseband component at $t=0$ during the data interval $-T < t < T$ to decide whether a_0 is +1 or -1. As mentioned in the previous section the contribution from the quadrature baseband component needs to be taken into account at the sampling instant of the inphase baseband component.

Thus the expression for the inphase baseband sample at $t=0$ during the data interval $-T < t < T$ can be written as [cf. Eqn. (2.11)]

$$x'(t_0) = f(R) \cos[\lambda(t_0) + \phi(R)] + n_c''(t_0) \quad (3.4)$$

where

$$R(t_0) = \sqrt{x^2(t_0) + y^2(t_0)}$$

$$\lambda(t_0) = \tan^{-1} [y(t_0)/x(t_0)]$$

$$x(t_0) = a_0 q(t_0) + \sum_{k=1}^H A_k(t_0) \cos \phi_k + n'_c$$

$$y(t_0) = q_I + \sum_{k=1}^H A_k(t_0) \sin \phi_k + n'_s$$

$$q_I = a_{-1} q(t_0 + T) + a_1 q(t_0 - T)$$

(3.5)

3.3 Probability of Bit Error

3.3.1 Conditional Probability of Bit Error

Initially, it is assumed that the quadrature components n'_c and n'_s of the uplink additive Gaussian noise, the cochannel interference and the interference from the quadrature baseband component q_I are known, and the probability of error of the inphase baseband bit decision conditioned on these random variables is determined. This expression for the probability of error, conditional on n'_c , n'_s , CCI random variables and q_I , is the same as in the case of MSK which is given in Eqn. (2.21) as

$$P'_e = \frac{1}{2} - \frac{1}{2} \operatorname{erf} \left[\frac{f(R) \cos \theta}{\sqrt{2 \sigma_d^2}} \right] \quad (3.6)$$

where $\theta = \lambda(t_0) + \phi(R)$ and σ_d is the uplink Gaussian noise power.

The conditioning on the random variables can be removed by taking the expectation of P_e over x and y which are defined in Eqn. (3.5). However, we need to first evaluate the joint probability density function $p(x,y)$ which is detailed in the next section.

3.3.2 Joint Probability Density Function $p(x,y/q_I)$

The evaluation of the joint PDF $p(x,y)$ can be done as follows. From Eqn. (3.5) the random variables x and y at the sampling instant $t=0$ may be written as

$$\begin{aligned} x &= a_0 q_0 + \alpha + n'_c \\ y &= q_I + \beta + n'_s \end{aligned} \quad (3.7)$$

where

$$\begin{aligned} q_I &= a_{-1} q_{-1} + a_1 q_1 \\ \alpha &= \sum_{k=1}^H A_k(t) \cos \phi_k \\ \beta &= \sum_{k=1}^H A_k(t) \sin \phi_k \end{aligned} \quad (3.8)$$

In Eqn. (3.8), q_I is the interference from the two consecutive quadrature baseband pulses a_{-1} and a_1 at the sampling instant $t=0$, and α and β are the cochannel interference due to $H(1,2 \dots \infty)$ interferers in the inphase and quadrature channels respectively. Since n'_c and n'_s are Gaussian random variables, the joint PDF of x and y conditional on the cochannel interference random variables α

and β , and the interference from quadrature baseband component q_I is obtained as

$$p(x, y/a, \beta, q_I) = \frac{1}{2\pi \sigma_u^2} \exp \left[-\left(\frac{x - q_0}{\sqrt{2} \sigma_u} \right)^2 \right] \\ \times \exp \left[-\left(\frac{y - q_I}{\sqrt{2} \sigma_u} \right)^2 \right] \quad (3.9)$$

where σ_u^2 is the variance of the quadrature components of the uplink noise. Using the generating functions $g(x, z)$ defined in Eqn. (2.24), the above equation can be expanded in the form of an infinite series. The details of the derivation were given in Chapter 2. The series expression for the conditional PDF is

$$p(x, y/a, \beta, q_I) = \frac{1}{2\pi \sigma_u^2} \exp \left[-\left(\frac{x - q_0}{\sqrt{2} \sigma_u} \right)^2 \right] \\ \times \exp \left[-\left(\frac{y - q_I}{\sqrt{2} \sigma_u} \right)^2 \right] \sum_{l, m} \left(\frac{1}{\sqrt{2} \sigma_u} \right)^{l+m} \frac{a^l \beta^m}{l! m!} \\ \times H_l \left(\frac{x - q_0}{\sqrt{2} \sigma_u} \right) H_m \left(\frac{y - q_I}{\sqrt{2} \sigma_u} \right) \quad (3.10)$$

The conditioning on the random variables a and β is removed by averaging $p(x, y/a, \beta, q_I)$ over the random variables a and β . The PDF $p(x, y/q_I)$ can therefore be expressed in terms of the moments of the CCI random variables as

$$\begin{aligned}
 p(x, y/q_I) = & \frac{1}{2\pi \sigma_u^2} \exp\left[-\left(\frac{x-q_0}{\sqrt{2} \sigma_u}\right)^2\right] \\
 & \times \exp\left[-\left(\frac{y-q_I}{\sqrt{2} \sigma_u}\right)^2\right] \sum_{l,m} \left(\frac{1}{\sqrt{2} \sigma_u}\right)^{l+m} \frac{E[\alpha^l \beta^m]}{l! m!} \\
 & \times H_l\left(\frac{x-q_0}{\sqrt{2} \sigma_u}\right) H_m\left(\frac{y-q_I}{\sqrt{2} \sigma_u}\right)
 \end{aligned} \quad (3.11)$$

The moments of the CCI random variables are evaluated from the joint characteristic function of the random variables α and β as described in Chapter 2 [Cf. Eqn. (2.43) to Eqn. (2.45)]. Therefore the required expression for $p(x, y/q_I)$ is obtained by substituting the value of $E[\alpha^l \beta^m]$ from Eqn. (2.48) in Eqn. (3.11).

3.3.3 Joint Probability Density Function $p(x, y)$

The unconditioned PDF $p(x, y)$ is obtained by averaging the conditional PDF $p(x, y/q_I)$ over the random variable q_I which is given in Eqn. (3.8) as

$$q_I = a_{-1} q_{-1} + a_1 q_1 \quad (3.12)$$

It is clear from Eqn. (3.12) that q_I depends upon the two consecutive quadrature bits a_{-1} and a_1 . If the two consecutive bits assume the value +1 as shown in Fig. 3.1(A), then the interference from the quadrature baseband component q_I is equal to q_0 at $t=0$. If the two consecutive bits assume the value -1 as shown in Fig. 3.1 (B), then the interference from the quadrature baseband component q_I is equal to $-q_0$ at

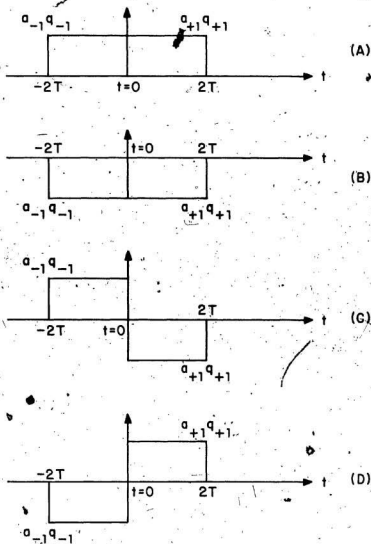


FIG. 3.1 BASEBAND WAVEFORM OF THE QUADRATURE CHANNEL FROM $t = -2T$ TO $t = 2T$.

the sampling instant $t=0$.

If the two consecutive bits assume the values +1 and -1 as in Fig. 3.1 (c) or -1 and +1 as in Fig. 3.1(D), then the interference from the quadrature baseband component q_I is equal to zero at the sampling instant $t=0$. Since the four possibilities that the two consecutive bits can assume have equal probability, the probability density function of q_I , $p(q_I)$, may be written as

$$p(q_I) = \frac{1}{4} \delta(q_I - 1) + \frac{1}{4} \delta(q_I + 1) + \frac{1}{2} \delta(q_I) \quad (3.13)$$

where $\delta(x)$ is the Dirac-delta function.

As mentioned before the PDF $p(x,y)$ is evaluated by taking the expectation of the conditional PDF $p(x,y/q_I)$ over the random variable q_I as

$$p(x,y) = \int_{-\infty}^{\infty} p(x,y/q_I) p(q_I) dq_I \quad (3.14)$$

Using the shifting property of dirac delta function, Eqn. (3.14) can be easily evaluated yielding

$$p(x,y) = \frac{1}{4} p(x,y/q_I = +1) + \frac{1}{4} p(x,y/q_I = -1) + \frac{1}{2} p(x,y/q_I = 0) \quad (3.15)$$

By substituting Eqn. (3.11) in Eqn. (3.15) we can obtain the required expression for the PDF $p(x,y)$.

3.3.4 Expression for Bit Error Probability

The final expression for the bit error rate (BER),

is obtained by evaluating the expectation of P'_e in Eqn. (3.6) using the PDF $p(x,y)$ given in Eqn. (3.15) as

$$P_e = \int_{-\infty}^{\infty} \int_{-\infty}^{\infty} P'_e(x,y) p(x,y) dx dy \quad (3.16)$$

Therefore by combining Eqn. (3.16) and Eqn. (3.15) the bit error probability may be expressed as

$$\begin{aligned} P_e &= \frac{1}{4} \int_{-\infty}^{\infty} \int_{-\infty}^{\infty} P'_e(x,y) p(x,y/q_I = q_0) dx dy \\ &+ \frac{1}{4} \int_{-\infty}^{\infty} \int_{-\infty}^{\infty} P'_e(x,y) p(x,y/q_I = -q_0) dx dy \\ &+ \frac{1}{2} \int_{-\infty}^{\infty} \int_{-\infty}^{\infty} P'_e(x,y) p(x,y/q_I = 0) dx dy \end{aligned} \quad (3.17)$$

By substituting Eqns. (3.6), (3.11), and (2.48) in Eqn. (3.17) we can write

$$\begin{aligned} P_e &= \frac{1}{2} \sum_{\alpha=-1}^{+1} \left(\frac{1}{2}\right)^{\alpha^2} \left[\frac{1}{4\pi \sigma_u^2} \sum_{l,m} b_{l,m} (-1)^{\frac{l+m}{2}} \left(\frac{1}{\sqrt{2} \sigma_u}\right)^{l+m} \right. \\ &\times \int_{-\infty}^{\infty} \int_{-\infty}^{\infty} \operatorname{erf} \left[\frac{f(R) \cos \theta}{\sqrt{2} \sigma_d} \right] H_l \left(\frac{x-q_0}{\sqrt{2} \sigma_u} \right) H_m \left(\frac{y-\alpha q_0}{\sqrt{2} \sigma_u} \right) \\ &\times \exp \left[-\left(\frac{x-q_0}{\sqrt{2} \sigma_u} \right)^2 \right] \exp \left[-\left(\frac{y-\alpha q_0}{\sqrt{2} \sigma_u} \right)^2 \right] dx dy \left. \right] \end{aligned} \quad (3.18)$$

The BER expression can be simplified by changing the variables x and y to r and s by using the relations

$$r = \frac{x - q_0}{\sqrt{2} \sigma_u} \quad \text{and} \quad s = \frac{y - a q_0}{\sqrt{2} \sigma_u} \quad (3.19)$$

Then the expressions for R and θ may be obtained as

$$R^2 = \{q_0^2[(r + \rho_u)^2 + (s - a\rho_u)^2]\}/\rho_u^2$$

$$\theta = \phi(R) + \tan^{-1} \left(\frac{s - a\rho_u}{r + \rho_u} \right) \quad (3.20)$$

where the uplink SNR $\rho_u^2 = q_0^2/2\sigma_u^2$. By substituting Eqns. (3.19) and (3.20) in Eqn. (3.18) we can obtain the simplified expression for the bit error rate as

$$P_e = \frac{1}{2} \sum_{a=-1}^{+1} \left(\frac{1}{2}\right)^a \left[\frac{1}{2} - \frac{1}{2\pi} \sum_{l,m} (-1)^{(l+m)/2} (\rho_u)^{l+m} \right. \\ \times \frac{b_{l,m}}{(q_0)^{l+m}} \int_{-\infty}^{\infty} \int_{-\infty}^{\infty} \operatorname{erf} \left[\rho_d \frac{f(R) \cos \theta}{\sqrt{f^2(R)}} \right] \\ \left. \times H_l(r) H_m(s) \exp[-(r^2 + s^2)] dr ds \right] \quad (3.21)$$

3.4 Probability of Bit Error in the Presence of Single Cochannel Interferer

In this section, we shall derive an expression for the bit error rate of QPSK signals when the signal is corrupted by single cochannel interferer in the uplink. For this purpose, the joint PDF of x and y conditioned on the

interference from quadrature baseband component q_I is obtained by using Eqn. (2.60) as

$$p(x, y/q_I) = \frac{1}{2\pi \sigma_u^2} \exp\left[-\left(\frac{x-q_0}{\sqrt{2} \sigma_u}\right)^2\right] \exp\left[-\left(\frac{y-q_I}{\sqrt{2} \sigma_u}\right)^2\right] \\ \times \exp\left[-\left(\frac{A}{\sqrt{2} \sigma_u}\right)^2\right] I_0(x) \quad (3.22)$$

where

$$x = \frac{\sqrt{2} A}{\sigma_u} \sqrt{\left(\frac{x-q_0}{\sqrt{2} \sigma_u}\right)^2 + \left(\frac{y-q_I}{\sqrt{2} \sigma_u}\right)^2} \quad (3.23)$$

In the above expressions, A is the amplitude of the CCI and σ_u^2 is the variance of the quadrature components of the uplink Gaussian noise. The PDF $p(x, y)$ may be obtained by the method illustrated in Section 3.3.3. By substituting Eqn. (3.15) in Eqn. (3.22) we can obtain the required expression for the PDF $p(x, y)$.

The expression for the bit error probability is then obtained by combining Eqns. (3.6), (3.15), and (3.22) as

$$\begin{aligned}
P_e = & \frac{1}{2} \sum_{a=-1}^{+1} \left(\frac{1}{2}\right)^a \left\{ \frac{1}{2} - \frac{1}{4\pi\sigma_u} \exp\left[-\left(\frac{A}{\sqrt{2}\sigma_u}\right)^2\right] \right. \\
& \times \int_{-\infty}^{\infty} \int_{-\infty}^{\infty} \operatorname{erf}\left[\frac{f(R) \cos \theta}{\sqrt{2}\sigma_d}\right] \\
& \times I_0\left[\frac{\sqrt{2}A}{\sigma_u} \sqrt{\left(\frac{x-q_0}{\sqrt{2}\sigma_u}\right)^2 + \left(\frac{y-aq_0}{\sqrt{2}\sigma_u}\right)^2}\right] \\
& \times \exp\left[-\left(\frac{x-q_0}{\sqrt{2}\sigma_u}\right)^2\right] \exp\left[-\left(\frac{y-aq_0}{\sqrt{2}\sigma_u}\right)^2\right] dx dy \Big\} \quad (3.24)
\end{aligned}$$

The above expression can be simplified by changing the variables x and y to r and s using the relations given in Eqns. (3.19) and (3.20) as

$$\begin{aligned}
P_e = & \frac{1}{2} \sum_{a=-1}^{+1} \left(\frac{1}{2}\right)^a \left\{ \frac{1}{2} - \frac{1}{2\pi} \exp\left[-\left(\frac{\rho_u A}{q_0}\right)^2\right] \right. \\
& \times \int_{-\infty}^{\infty} \int_{-\infty}^{\infty} \operatorname{erf}\left[\rho_d \frac{f(R) \cos \theta}{\sqrt{f^2(R)}}\right] \\
& \times I_0\left[\frac{2\rho_u A}{q_0} \sqrt{r^2+s^2}\right] \exp[-(r^2+s^2)] dr ds \Big\} \quad (3.25)
\end{aligned}$$

3.5 Probability of Bit Error in the Absence of Cochannel Interference

When there is no cochannel interference, the signal will be distorted by Gaussian noise only and the corresponding expression for the bit error probability is obtained by using the PDF $p(x,y)$ as explained below. The

joint PDF of x and y conditioned on the quadrature baseband component q_I in the absence of cochannel interference is obtained from Eqn. (3.9) by setting α and β to zero, whence

$$p(x, y/q_I) = \frac{1}{2\pi \sigma_u^2} \exp\left[-\left(\frac{x-q_0}{\sqrt{2} \sigma_u}\right)^2\right] \exp\left[-\left(\frac{y-q_I}{\sqrt{2} \sigma_u}\right)^2\right] \quad (3.26)$$

The conditioning on q_I is removed by using the method described in Section 3.3.3 and the required expression for the PDF $p(x, y)$ is obtained by substituting Eqn. (3.15) in Eqn. (3.26). The desired BER expression in the absence of cochannel interference is derived by combining Eqns. (3.6), (3.15) and (3.26) as

$$P_e = \frac{1}{2} \int_{\alpha=-1}^{+1} \left(\frac{1}{2}\right)^{\alpha^2} \left\{ \frac{1}{2} - \frac{1}{4\pi \sigma_u^2} \int_{-\infty}^{\infty} \int_{-\infty}^{\infty} \operatorname{erf}\left[\frac{f(R) \cos \theta}{\sqrt{2} \sigma_d}\right] \right. \\ \left. \times \exp\left[-\left(\frac{x-q_0}{\sqrt{2} \sigma_u}\right)^2\right] \exp\left[-\left(\frac{y-aq_0}{\sqrt{2} \sigma_u}\right)^2\right] dx dy \right\} \quad (3.27)$$

The above expression is simplified by changing the variables x and y to r and s using the relations given in Eqn. (3.19) and (3.20) as

$$P_e = \frac{1}{2} \int_{\alpha=-1}^{+1} \left(\frac{1}{2}\right)^{\alpha^2} \left\{ \frac{1}{2} - \frac{1}{2\pi} \int_{-\infty}^{\infty} \int_{-\infty}^{\infty} \operatorname{erf}\left[\rho_d \frac{f(R) \cos \theta}{\sqrt{f^2(R)}}\right] \right. \\ \left. \times \exp[-(r^2+s^2)] dr ds \right\} \quad (3.28)$$

3.6 Gaussian Approximation

Assuming that the cochannel interference is due to a Gaussian noise source, the performance of OQPSK signals in the presence of CCI can be approximated by using the expression derived for the error rate performance in the absence of CCI. The BER expression for this approximation is obtained from Eqn. (3.27) by changing the uplink noise power σ_u^2 to σ^2 where σ^2 is the sum of the Gaussian noise power σ_u^2 and the cochannel interference power σ_k^2 . The equivalent CCI power σ_k^2 is obtained as described in Section 2.7.

CHAPTER 4

NUMERICAL INVESTIGATIONS AND RESULTS4.1 Introduction

In this chapter, a numerical investigation of the BER expressions derived in Chapter 2 and Chapter 3 for MSK and QPSK signalling are presented. The transmission channel nonlinearity is modelled as a hard-limiting repeater and a satellite repeater and the investigation of each model is carried out. The bit error rates are computed when the signals are corrupted by a single CCI and multiple CCI's and are presented in graphical form. The error performance curves in the absence of cochannel interference are also presented.

4.2 Channel Models4.2.1 Travelling Wave Tube Model

The amplitude and phase nonlinearities observed in actual TWT amplifiers can be represented using the model given by Thomas et al. (1974). The analytical expression for AM/AM nonlinearity according to this model is

$$f(R) = \begin{cases} 10^{\alpha[\cos[\log_{10}(R/R)] - 1]} & R > \bar{R} \\ R & R < \bar{R} \end{cases} \quad (4.1)$$

where R denotes the amplitude of the input voltage corresponding to saturation and α , β and \bar{R} are constants

chosen to fit the data. The model given by Berman and Mahle (1970), after modifying some constants as suggested by Thomas et al. (1974), can be used to represent the AM/PM nonlinearity. The functional form of AM/PM nonlinearity is

$$\phi(R) = K_1[1 - \exp(-K_2 R^2)] + K_3 R^2 \quad (4.2)$$

where K_1 , K_2 and K_3 are constants chosen to fit measured data. The AM/AM and AM/PM characteristics of TRW DSC II satellite transponder is shown in Fig. 4.1 [Thomas et al. (1974)]. For this transponder, the values for the constants, are obtained as $\alpha=0.394$, $\beta = 0.475$, $\bar{R}=0.355$, $R=2.317$, $K_1=0.602$, $K_2=0.66$, $K_3=1/102.4$. We shall use the above transponder characteristics for numerical evaluation of the error rates in Section 4.5.

4.2.2 Hard-Limiter Model

In power-limited channels, it is desirable to operate the TWT amplifier in the saturation region in order for maximum utilization of the available power. In this region, the amplitude nonlinearity exhibit hardlimiting type characteristic. Therefore, if one neglects the phase nonlinearity assuming that the receiver can compensate for the phase distortion, transponder AM/AM conversion effect can be modelled by a hardlimiter whose input-output characteristic is

$$f(R) = \begin{cases} a & R > 0 \\ -a & R < 0 \end{cases} \quad (4.3)$$

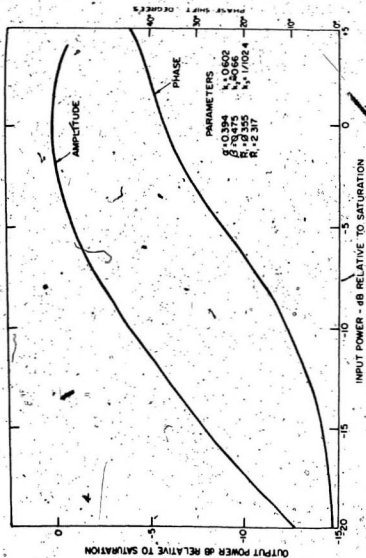


FIG. 4.1 PHASE AND AMPLITUDE CHARACTERISTICS OF TWT [THOMAS et al.(1974)]

where a is the clipping voltage. This transfer characteristic is shown in Fig. 4.2. The AM/PM conversion of a hard-limiter is zero for all R .

4.3 Computational Details

The numerical evaluation of the error rate expressions derived in Chapters 2 and 3 involves computation of Hermite polynomials, Bessel function, 'erf' function and double integrals. Also, it is required to expand the characteristic function of the CCI random variables in a power series. The purpose of this section is to describe the techniques used in computations, in detail.

4.3.1 General

The Hermite polynomials obey the recurrence relationship

$$H_{n+1}(x) - 2x H_n(x) + 2n H_{n-1}(x) = 0$$

$$n=1, 2, \dots \quad (4.4)$$

A computer programme is written for recursive computation of Hermite polynomials using the above formula. The values, $H_0(x)=1$ and $H_1(x)=2x$ are used for initiating the recursive procedure, for a given argument x . The program is tested using the known values of Hermite polynomials.

In Chapters 3 and 4, we have seen that it is necessary to expand the characteristic function of the CCI

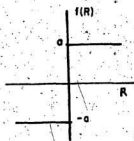


FIG. 4.2 HARD-LIMITER TRANSFER FUNCTION

random variables in a power series in order to compute the error rates. The power series expansion is obtained by employing the series multiplication formulas as outlined in Appendix A. A computer program that can perform multiplication of H power series is written and used for obtaining the required coefficient of the power series expansion of the characteristic function. Since this multiplication involves multiplication of H number of Bessel functions, the accuracy of the program is verified by comparing with the known values of the Bessel function of the order zero given by Abramowitz and Stegun (1972).

The modified Bessel function of the first kind of the order zero, $I_0(X)$, is computed using the double precision version of the IMSL subroutine 'MMBSIO'. The error function $\text{erf}(x)$ is evaluated using the double precision IMSL subroutine 'DERF'.

The double integrals in bit error rate expressions are numerically evaluated using Cartesian products of Gauss-Hermite quadrature formulas. Spot checks are made with computations of the double integrals using the double precision version of the IMSL subroutine 'DBLIN' and the convergence is obtained up to three significant digits.

For error rates greater than 10^{-6} , 34 and 47 point quadrature formulas provide convergence up to three significant digits. For the error rates in the range 10^{-6} to

10^{-12} , the 47 and 52 point quadrature formulas give results identical to three significant digits. Therefore the 47 point quadrature formula is judged sufficient in our range of investigation.

In all our computations we have found that the infinite series can be terminated after 24 terms providing accuracy up to three significant digits. In other words, the number of terms of the double series considered are $l=24$ and $m=24$.

4.3.2 Downlink Carrier Power

The average value of the downlink carrier power, $f^2(R)$, in the BER expressions is computed by averaging $f^2(R)$ over the random variables x and y

$$\overline{f^2(R)} = E[f^2(\sqrt{x^2+y^2})] = \int_{-\infty}^{\infty} \int_{-\infty}^{\infty} f^2(\sqrt{x^2+y^2}) p(x,y) dx dy \quad (4.5)$$

By substituting the value of $p(x,y)$ from Eqn. (2.32) the above equation can be written as

$$\begin{aligned} \overline{f^2(R)} = & \int_{-\infty}^{\infty} \int_{-\infty}^{\infty} f^2(\sqrt{x^2+y^2}) \frac{1}{2\pi\sigma_u^2} \exp\left[-\left(\frac{x-q_0}{\sqrt{2}\sigma_u}\right)^2\right] \\ & \times \exp\left[-\left(\frac{y}{\sqrt{2}\sigma_u}\right)^2\right] I_{l,m}\left(\frac{1}{\sqrt{2}\sigma_u}\right)^{l+m} (-1)^{(l+m)/2} b_{l,m} \\ & \times H_l\left(\frac{x-q_0}{\sqrt{2}\sigma_u}\right) H_m\left(\frac{y}{\sqrt{2}\sigma_u}\right) dx dy \quad (4.6) \end{aligned}$$

The above equation is simplified by changing the variables x

and y to r and s using the relations $r=(x-q_0)/\sqrt{2} \sigma_u$ and $s=y/\sqrt{2} \sigma_u$, whence

$$\begin{aligned} \overline{f^2(R)} = & \frac{1}{\pi} \sum_{l,m} (-1)^{(l+m)/2} (\rho_u)^{l+m} \frac{b_{l,m}}{(q_0)^{l+m}} \\ & \times \int_{-\infty}^{\infty} \int_{-\infty}^{\infty} f^2(R) H_l(r) H_m(s) \exp[-(r^2+s^2)] dr ds \end{aligned} \quad (4.7)$$

where $R^2 = [q_0^2[(r+\rho_u)^2 + s^2]]/\rho_u^2$

The values computed from the above expression are used to obtain the bit error rates for various uplink and downlink signal to noise power ratios. These bit error rates are compared with the bit error rates obtained by approximating $f^2(R)$ as $f^2(q_0)$. These are tabulated in Table 4.1. From this comparison it is clear that $\overline{f^2(R)}$ can be approximated by $f^2(q_0)$. The advantage is significant saving in the computational effort.

4.4 Performance of MSK and QPSK Signals in the Absence of CCI

Bit error rates of MSK signals in the absence of cochannel interference are computed and plotted in Fig. 4.3 for a hard-limited channel. In all these figures, the vertical axis represents the logarithmic value of the bit error rate and the horizontal axis represents the downlink signal to noise power ratio in decibels. Identical markers

Table 4.1 Comparison of BER's of MSK, through TWT channel with backoff 0 dB, computed using $\overline{f^2(R)}$, without approximation and with approximation to $f^2(q_0)$

Uplink SNR in dB	Downlink SNR in dB	BER (using approximation $\overline{f^2(R)} = f^2(q_0) = 1$)	Exact value of $\overline{f^2(R)}$	BER (using exact value $\overline{f^2(R)}$)
9	10	0.353×10^{-3}	0.954	0.329×10^{-3}
9	12	0.210×10^{-3}	0.954	0.203×10^{-3}
12	10	0.153×10^{-4}	0.926	0.130×10^{-4}
12	12	0.163×10^{-5}	0.976	0.152×10^{-5}
15	10	0.564×10^{-5}	0.988	0.500×10^{-5}
18	10	0.456×10^{-5}	0.994	0.429×10^{-5}
21	10	0.418×10^{-5}	0.996	0.405×10^{-5}

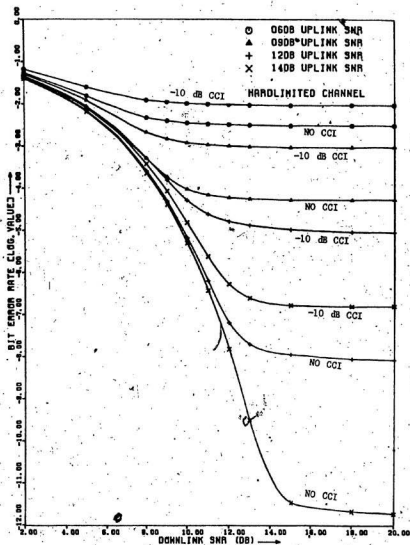


FIG. 4.3 BIT ERROR PROBABILITY OF MSK SIGNALS;
HARD-LIMITED CHANNEL, CCI -10 dB.

are used to indicate the curves showing the error performance in the presence of and absence of CCI but having the same uplink SNR. The error rates are plotted against the downlink SNR, keeping uplink SNR as a parameter. The four curves designated 'NO CCI' are computed for the uplink SNR values 6dB, 9dB, 12 dB and 14 dB, assuming that there is no cochannel interference in the uplink. It is evident from these curves that as we increase the downlink SNR the error rate decreases and approaches a constant value. These error rates were found to be in good agreement with the published error performance curves of Jain and Blachman (1973).

Similarly, the bit error rates of QPSK signals in the absence of cochannel interference are computed and plotted in Fig. 4.4 for hard-limited channel for the same uplink SNR values as in Fig. 4.3. The behaviour of the curves is the same as in the case of MSK signals. These error rates are compared with those obtained by Ekanayake (1983) for QPSK signals under the influence of intersymbol interference for a hard-limited channel and found to be within the acceptable limits.

4.5 Performance of MSK and QPSK Signals in the Presence of One CCI

4.5.1 Hard-limited Channel

The bit error rates of MSK signals in the presence

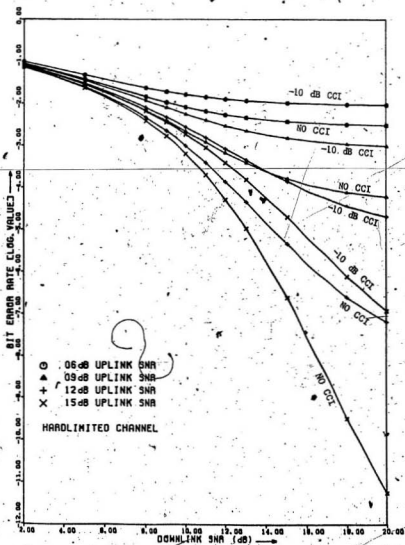


FIG. 4.4 BIT ERROR PROBABILITY OF QPSK SIGNALS;
HARD-LIMITED CHANNEL, CCI -10 dB.

of single CCI are computed using both the series expression (2.54) and the expression without power series given by (2.63). The results obtained by the two methods are identical up to 8 significant digits. The performance curves are obtained for the uplink SNR values 6 dB, 9 dB, 12 dB and 14 dB. The four curves designated '-10 dB CCI' represent the error performance under the influence of single CCI of interference power -10 dB relative to the signal power.

The bit error rates of QPSK signals in the presence of single CCI are computed by using both the series expression given in Eqn. (3.21) and the non-series expression given in Eqn. (3.25). The values obtained by the two methods are identical up to 8 significant digits. The error performance curves are obtained for the same uplink SNR parameters as in the previous case and shown in Fig. 4.4. The interference power is assumed to be -10 dB relative to the signal power. It is evident from Figure 4.3 and 4.4 that for low uplink SNR the error rate decreases slowly and finally reaches a constant value at relatively lower values of downlink SNR. As we increase the uplink SNR the error rate decreases rapidly and reaches a constant value but for relatively higher values of the downlink SNR. By comparing Figures 4.3 and 4.4 it can be observed that the performance of MSK is superior to QPSK for all the values of uplink and downlink SNR's.

4.5.2 TWT Channel

In this section we investigate the effect of TWT input power backoff from the saturation region on the bit error performance of MSK and QPSK signals. The AM/AM and AM/PM conversion effects of various TWT operating points are investigated by using the model explained in Section 4.2. In the present investigation the receiver is considered to be a phase compensated type as explained below. When the uplink noise and interference are absent, the AM/PM nonlinearity will result in a phase shift $\phi(A)$, where A is the envelope of the input signal to the TWT. But in the presence of noise and interference, the phase distortion $\phi(R)$ introduced by the TWT will be different from $\phi(A)$ and varies randomly with time. In a phase compensated receiver it is assumed that the receiver is designed so that it subtracts the constant phase shift $\phi(A)$ from the instantaneous phase distortion $\phi(R)$. That is, the overall AM-PM conversion is $\phi(R) - \phi(A)$.

When the TWT is operated at the saturation region it is referred to as the input power backoff 0 dB. This is accomplished by setting the operating voltage R to \hat{R} which is equal to 2.317 as given in Fig. 4.1. In order to operate the TWT in the linear region, input voltage needs to be reduced below R , and this case is generally referred to as input 'power backoff'. The input power backoff value is given as $20 \log_{10}(R/\hat{R})$ where R is the input voltage.

Figures 4.5 to 4.8 show the error curves of MSK signals for TWT input power backoff 0 dB, -2dB, -4 dB and -6dB. In each figure there are four error curves obtained in the absence of CCI for the same uplink SNR parameters mentioned before. The corresponding error rate curves in the presence of single CCI of interference power -10 dB is also shown in each of the aforementioned figures. When the uplink SNR is small, the error rate decreases slowly as we increase the downlink SNR. Also, the error rate tends to bottom off for relatively low values of downlink SNR. Under this condition the error rate is solely influenced by the uplink noise and interference and the channel is said to be uplink limited. On the other hand, when the uplink SNR is high, the error rate decreases rapidly as we increase the downlink SNR and tends to bottom off at high values of downlink SNR. This effect can be explained by the fact that the downlink noise becomes important in its effect on the error rate at high uplink SNR and the channel may be considered as downlink limited.

The effect of TWT input power backoff affects the bit error performance in two ways. Backoff from the saturation causes the TWT to operate in the linear region where the amplitude dependent phase shift is relatively small. Thus one would expect error rate to be lower in the linear region. However, the input power backoff reduces both

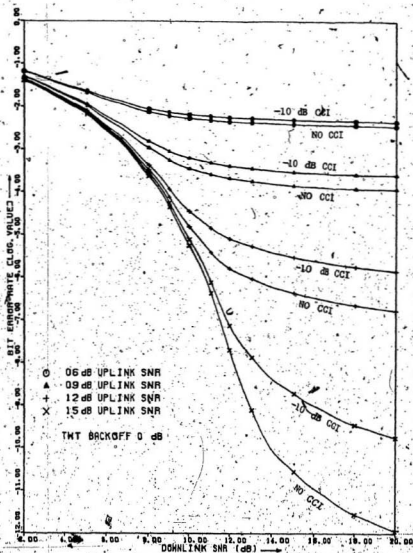


FIG. 4.5 BIT ERROR PROBABILITY OF MSK SIGNALS;
TWT CHANNEL, CCI-10dB, BACKOFF 0 dB.

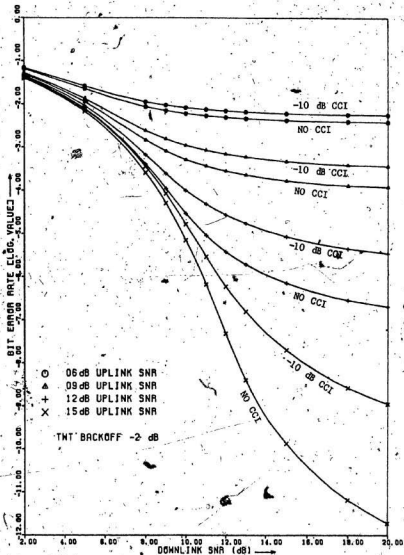


FIG. 4.6 BIT ERROR PROBABILITY OF MSK SIGNALS;
TWT CHANNEL, CCI-10dB, BACKOFF -2 dB.

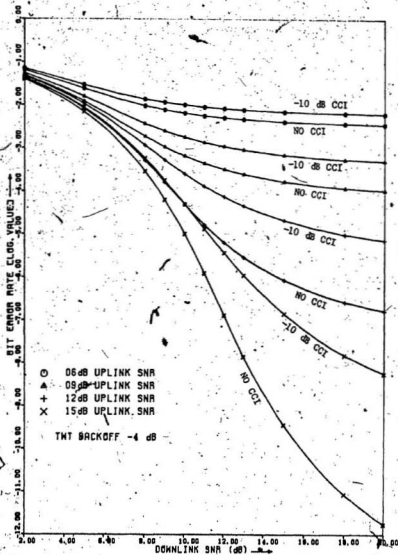


FIG. 4.7 BIT ERROR PROBABILITY OF MSK SIGNALS;
TWT CHANNEL, CCI -10dB, BACKOFF -4dB.

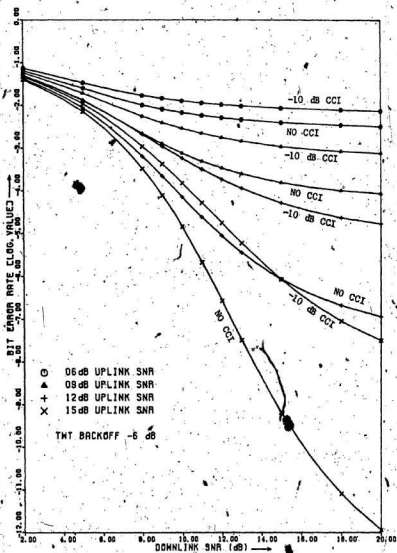


FIG. 4.8 BIT ERROR PROBABILITY OF MSK SIGNALS;
TWT CHANNEL, CCI -10 dB, BACKOFF -6 dB.

uplink and downlink SNR's and causes an increase in error rate.

From Figures 4.5 to 4.8 it can be observed that as we increase the backoff and operate in the linear region the error rate increases for all uplink and downlink SNR's. As explained before, this is because of the reduction in AM/PM conversion effect due to the TWT input power backoff which has much less effect on the error rate in a phase compensated receiver. The reduction in the uplink and downlink SNR will be the predominant factor as we increase the TWT input power backoff, thereby causing higher error rates.

The effect of the input power backoff on the error performance of QPSK signals are shown in Figures 4.9 to 4.12. In each figure there are four curves showing the error performance in the absence of CCI and another four curves showing the performance under the influence of CCI. As before, the results show that the error rate performance degrades as we increase the TWT input power backoff for all the values of uplink and downlink SNR's.

Thus we can conclude that, from the point of view of error performance, it is desirable to operate the TWT amplifier at saturation for all uplink and downlink SNR's. This conclusion is valid for both MSK and QPSK signalling schemes. By comparing the MSK and QPSK error performance curves in Figures 4.5 to 4.12 one can note that MSK has lower

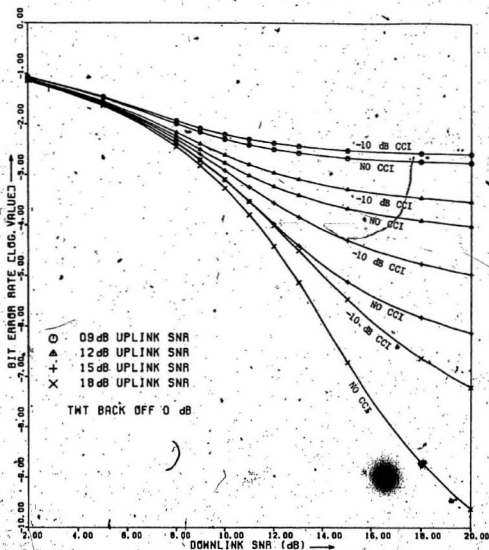


FIG. 4.9 BIT ERROR PROBABILITY OF QPSK SIGNALS,
TWT CHANNEL, CCI -10 dB, BACKOFF 0 dB.

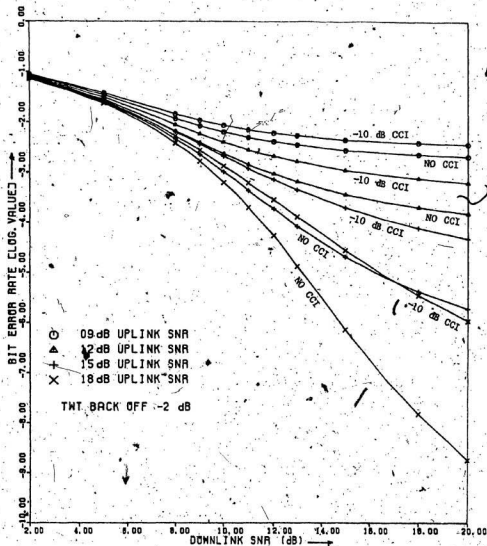


FIG. 4.10 BIT ERROR PROBABILITY OF OQPSK SIGNALS;
TWT CHANNEL, CCI -10 dB, BACKOFF -2 dB.

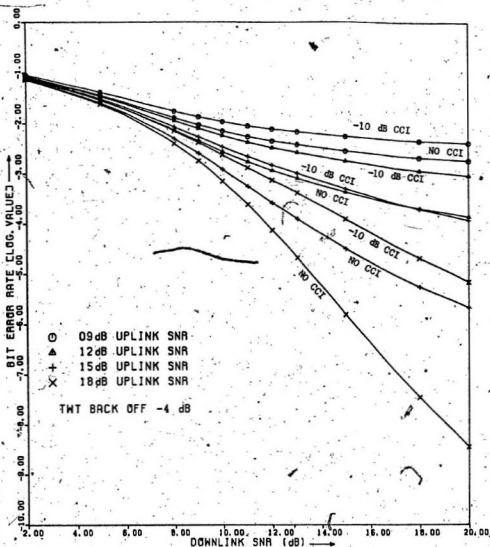


FIG. 4.11 BIT ERROR PROBABILITY OF OQPSK SIGNALS;
TWT CHANNEL, CCI-10 dB, BACKOFF -4 dB.

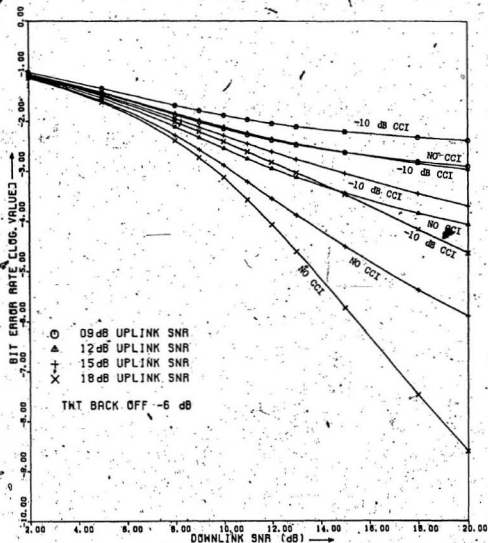


FIG. 4.12 BIT ERROR PROBABILITY OF OQPSK SIGNALS;
TWT CHANNEL, CCI-10 dB, BACKOFF -6 dB.

error rates than QPSK at all the input power backoff values.

4.5.3 Comparison of Hard-Limiter Model and TWT Model

In this section we compare the error performance of MSK and QPSK signals transmitted through a hard-limited channel and a TWT channel. The TWT input power backoff is assumed to be 0 dB.

By comparing the performance of MSK signals through the two models shown in Fig. 4.3 and Fig. 4.5, it can be observed that for low uplink SNR (< 12 dB) the hard-limiter model provides nearly the same result compared to the TWT model. But for high uplink SNR (> 12 dB) the hard-limiter model is found to yield high error rates. The same conclusion can be made for QPSK signals by comparing Figures 4.4 and 4.6. Therefore the hard-limiter model can provide reasonably accurate error rate estimates at low uplink SNR for both MSK and QPSK signals. For high uplink SNR, it provides an upper bound on the performance.

4.6 Error Performance in the Presence of Multiple Cochannel Interferers

4.6.1 Exact Method

The bit error rate of MSK signals transmitted through a hard-limited channel is computed using the series expression given in Eqn. (2.54) for various equal power cochannel interferers. The interference power of the CCI is

assumed to be -20 dB to obtain the performance curves in a proper range for all the parameters. Fig. 4.13 shows the error performance curves of MSK signals when the uplink SNR is 14 dB. These error rates are computed assuming the MSK signals are affected by several equal power cochannel interferers.

As it is expected, the error performance degrades as we increase the number of cochannel interferers affecting the signal. The computation time required for error rate calculation grows rapidly with the increase of the number of interferers. In the following section, we compare the results with those obtained by an approximate technique, which requires comparatively less computation time.

4.6.2 Gaussian Approximation Method

The bit error rates of MSK signals transmitted through a hard-limited channel are computed using the expressions (2.74 and (2.75) for various equal power cochannel interferers. The error performance curves are obtained for the same parameters as in the exact method and shown in Fig. 4.14.

By comparing Figures 4.13 and 4.14 one can note that for low downlink SNR (< 10 dB), the Gaussian approximation method gives almost the same error rates as the exact method. For high downlink SNR's (> 10 dB) the approximation method yields slightly higher error rate than

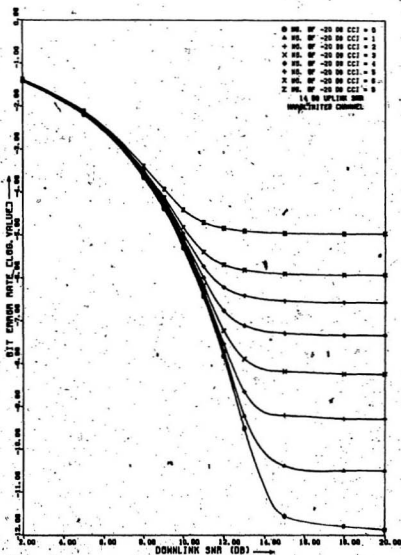


FIG. 4.13 EXACT BIT ERROR PROBABILITY OF MSK IN THE PRESENCE OF MULTIPLE CCI; HARD-LIMITED CHANNEL, CCI -20 dB.

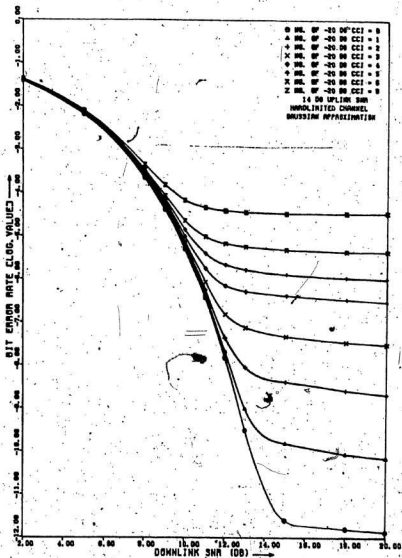


FIG. 4.14 APPROXIMATE BIT ERROR PROBABILITY OF MSK
IN THE PRESENCE OF MULTIPLE CCI,
HARD-LIMITED CHANNEL, CCI -20 dB.

the exact method for all uplink SNR values. But as the number of cochannel interferers increase, the difference in error rates of the two methods decreases. Therefore if the number of interferers is large the Gaussian approximation method can provide reasonably accurate bit error rate values.

CHAPTER 5

CONCLUSION5.1 Contributions of This Thesis

In this thesis we have investigated the error performance of MSK and QPSK signals which have been transmitted through a two-link nonlinear satellite channel. Both hard-limited and TWT channel models have been considered in the analysis. The effect of Gaussian noise in both the uplink and the downlink has been considered but the cochannel interference has been assumed to be present only in the uplink. The amplitude and phase nonlinearity of the TWT amplifier has been taken into account in the analysis. As the result of the investigation, the contributions made are outlined below.

Firstly, the bit error rate expressions for both MSK and QPSK signals under the influence of multiple cochannel interferers have been derived in the form of an infinite series which are valid for both hard-limited as well as for TWT channel models. Secondly, alternative expressions for performance evaluation of MSK and QPSK signals in the presence of single cochannel interferer have been derived. These expressions do not contain infinite series and therefore the computation can be done efficiently. Thirdly, BER expressions in the absence of cochannel interference have

been obtained for the two signalling techniques. Finally, a simple expression which can be computed more efficiently than the expression which contain infinite series has been derived by approximating the CCI to an equivalent Gaussian noise source.

The numerical results for the error rate of the two signalling schemes have been presented for both hard-limited and TWT channel models. The time required for all the error rate computations were found to be moderate.

The effect of TWT input power backoff from saturation on the error rate was investigated numerically for both MSK and OQPSK signals. The optimum operating region was found to be the saturation region for all uplink and downlink signal to noise power ratios for both MSK and OQPSK signalling techniques.

The effect of multiple cochannel interferers has been investigated only for MSK signals. The channel model in this case was assumed to be a hard-limiter. The numerical results were computed using the power series method as well as the Gaussian approximation method. The Gaussian approximation method was found to yield accurate results for low (< 10 dB) downlink SNR's. However the results indicate that the Gaussian approximation method is reasonably valid even for high downlink signal to noise power ratios when the number of interferers is high.

From the numerical investigation of the two signalling techniques it is concluded that MSK is superior to OQPSK under all signal and noise conditions. The performance degradation of OQPSK signals can be explained from the fact that there is an interference from the quadrature baseband component at the sampling instant of the inphase baseband component due to its rectangular pulse shaping. Also we have found that the hard-limiter model is a good replacement for TWT model at low uplink SNR for both signalling techniques.

5.2 Recommendations for Further Research

In the present study we have not considered the effect of intersymbol interference caused by the transmitted filters, satellite filters and receiver filters. In practice all these filters cause signal distortion and in turn cause performance degradation. A detailed analysis of the effect of CCI and intersymbol interference, introduced in both the uplink and the downlink, on the error performance would be a significant and useful contribution to the satellite communication field.

In our investigation we have assumed perfect phase and timing synchronization. But in practice both phase and timing jitter are to be expected. Both these effects can be taken into account if the following assumptions are made. The distributions of these random processes are known and

they are independent of the other random processes in the system. Then by using the conditioning method illustrated in Section 2.4 the expression for the bit error rate can be obtained.

REFERENCES

- Abramowitz, M. and I. A. Stegun(1972), Handbook of Mathematical Functions, Dover, New York.
- Berman, A. L. and C. E. Mahle (1970), Nonlinear Phase Shift in Travelling-Wave Tubes as Applied to Multiple Access Communications Satellites, IEEE Trans. Commun. Tech., Vol. COM-18, pp. 37-48.
- Cruz, J. R., and R. S. Simpson (1981), Cochannell and Intersymbol Interference in Quadrature-Carrier Modulation Systems, IEEE Trans. Commun., Vol. COM-29, pp. 285-297.
- Ekanayake, N. (1983), MSK and Offset QPSK Signal Transmissions through Nonlinear Satellite Channels in the Presence of Intersymbol Interference, IEE Proc., Vol. 130, Part F, pp. 513-518.
- Forsey, R. J., V. E. Gooding, P. J. Mclane and L. L. Campbell (1978), M-ary PSK Transmission via a Coherent Two-Link Channel Exhibiting AM-AM and AM-PM Nonlinearities, IEEE Trans. Commun., Vol. COM-26, pp. 116-123.
- Gould, R. G. and Y. F. Lum (1975), Communications Satellite Systems: An Overview of the Technology, IEEE Press, New York.
- Gradshteyn, I. S., and I. W. Ryzhik (1965), Table of Integrals, series and products, Academic Press, New York.
- Gronemeyer, S. A. and A. L. McBride (1976), MSK and Offset QPSK Modulation, IEEE Trans. Commun., Vol. COM-24, pp. 809-819.
- Huang, T. C., J. K. Omura, and W. C. Lindsey (1981), Analysis of Coherent Satellite Communication Systems in the Presence of Interference and Noise, IEEE Trans. Commun., Vol. COM-29, pp. 593-604.
- Jain, P. C. (1972), Limiting of Signals in Random Noise, IEEE Trans. Inform. Theory, Vol IT-18, pp. 332-340.
- Kennedy, D. J. and O. Shimbo (1981), Cochannell Interference in Nonlinear QPSK Satellite System, IEEE Trans. Commun., Vol. Com-29, pp. 582-592.

- Mathews, N. A. and A. H. Aghvami (1980), M-ary CPSK Signalling over Two-Link Nonlinear Channels in Additive Gaussian Noise, IEE Proc., Vol. 127, Part F, pp. 410-414.
- Mathews, N. A. and A. H. Aghvami (1981), Binary and Quaternary CPSK Transmissions through Nonlinear Channels in Additive Gaussian Noise and Cochannel Interference, IEE Proc., Vol. 128, Part F, pp. 96-103.
- Pasupathy, S. (1979), Minimum Shift Keying: A Spectrally Efficient Modulation, IEEE Commun. Magazine, pp. 14-22.
- Shimbo, O. and R. Fang (1973), Effects of Cochannel Interference and Gaussian Noise in M-ary PSK Systems, Comsat Tech. Reveiw, Vol. 3, pp. 183-206.
- Thomas, C. M., M. Y. Weidner, and S. H. Durrani (1974), Digital Aplitude-Phase Keying with M-ary Alphabets", IEEE Trans. Commun., Vol. COM-22, pp. 168-180.

APPENDIX A

This appendix deals with the expansion of the joint characteristic function $\phi(u, v)$ given in Eqn. (2.45) in a power series.

The joint characteristic function of the CCI random variables α and β is reproduced from Eqn. (2.45) as

$$\phi(u, v) = \prod_{k=1}^H J_0(A_K \sqrt{u^2 + v^2}) \quad (A.1)$$

The Bessel function of the first kind of order zero in the above equation can be expanded in a two dimensional power series [Abramowitz and Stegun (1974)] as

$$J_0(A_K \sqrt{u^2 + v^2}) = \sum_{s=0}^{\infty} \sum_{t=0}^s \frac{(-1)^s}{(s!)^2} \left(\frac{A_K}{2}\right)^{2s} \\ \times \frac{s!}{(s-t)! t!} v^{2t} u^{(2s-2t)} \quad (A.2)$$

Therefore we can write

$$\phi(u, v) = \prod_{k=1}^H \sum_{\ell=0}^{\infty} \sum_{m=0}^{\infty} b_{\ell, m} u^{\ell} v^m \quad (A.3)$$

The coefficient $b_{\ell, m}$ for even values of ℓ and m is obtained from Eqn. (A.2) as

$$b_{\ell, m} = \frac{(-1)^{(\ell+m)/2} \left(\frac{A_K}{2}\right)^{\ell+m}}{\left(\frac{\ell+m}{2}\right)! \left(\frac{\ell}{2}\right)! \left(\frac{m}{2}\right)!} \quad (A.4)$$

The multiplication of the two dimensional power series can be done by using the formula given by Gradshteyn and Ryzhik (1965) as

$$\sum_{\ell=0}^{\infty} \sum_{m=0}^{\infty} A_{\ell,m} x^{\ell} y^m \sum_{\ell=0}^{\infty} \sum_{m=0}^{\infty} B_{\ell,m} x^{\ell} y^m = \sum_{\ell=0}^{\infty} \sum_{m=0}^{\infty} C_{\ell,m} x^{\ell} y^m \quad (\text{A.5})$$

where

$$C_{\ell,m} = \sum_{i=0}^{\ell} \sum_{j=0}^m A_{i,j} B_{\ell-i,m-j} \quad (\text{A.6})$$

By using the formulas given in Eqns. (A.5) and (A.6) repeatedly we can obtain the product of H two-dimensional power series.

